

Object Detection

- where is the object? And how many of them are there?

Milan Straka

📅 March 25, 2024



Charles University in Prague
Faculty of Mathematics and Physics
Institute of Formal and Applied Linguistics



unless otherwise stated

Beyond Image Classification

Beyond Image Classification

- Object detection
(including location)

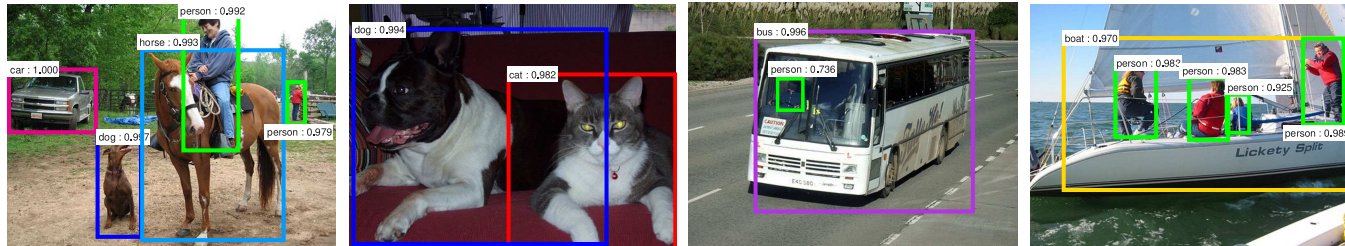


Figure 3 of "Faster R-CNN: Towards Real-Time Object Detection with Region Proposal Networks", <https://arxiv.org/abs/1506.01497>

- Image segmentation

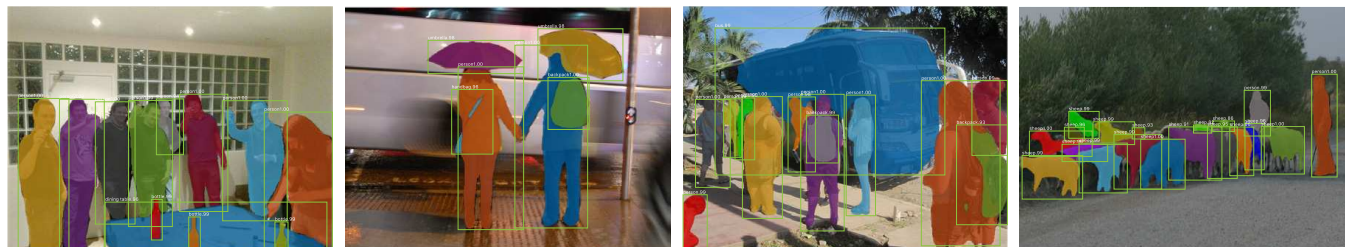


Figure 2 of "Mask R-CNN", <https://arxiv.org/abs/1703.06870>

- Human pose estimation



Figure 7 of "Mask R-CNN", <https://arxiv.org/abs/1703.06870>

Beyond Image Classification

Semantic Segmentation



CAT GRASS
TREE

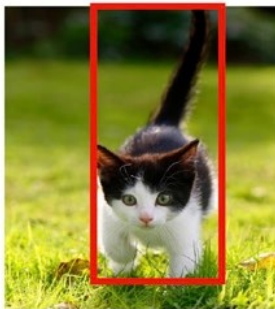
No object
Just pixels

Classification



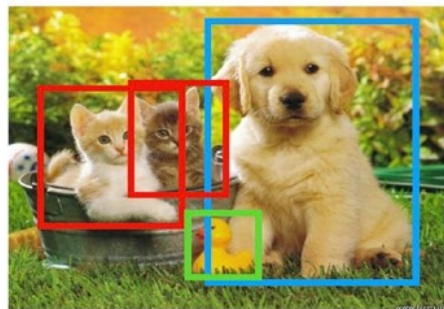
CAT

Classification + localization



CAT

Object detection



CAT DOG DUCK

Instance segmentation

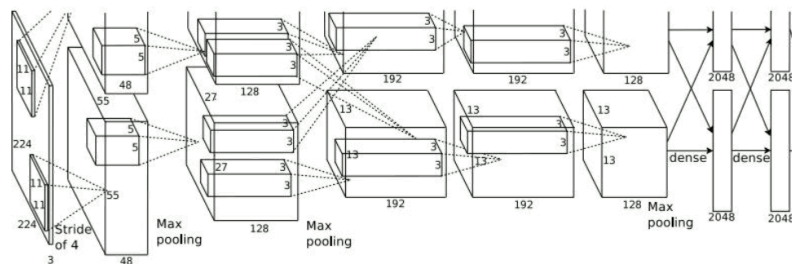
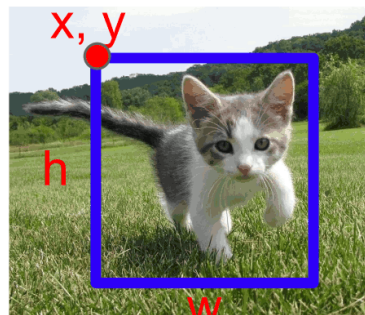


CAT CAT DOG DUCK

Single object

Multiple objects

<https://www.implantology.or.kr/articles/xml/RvNO/>



Fully Connected:
4096 to 1000

Class Scores

Cat: 0.9
Dog: 0.05
Car: 0.01
...

↳ klasichni klasiifikatsii

↳ boxovani

Vector: 4096
Fully Connected:
4096 to 4

Box Coordinates
(x, y, w, h)

*box
"bounding box"*

Slide 38 of http://cs231n.stanford.edu/slides/2021/lecture_15.pdf.

We can perform object localization by jointly predicting the bounding box coordinates using regression.

To be able to recognize and localize *several* objects, assume we were given multiple interesting regions of the image, called **regions of interest (RoI)**. For each of them, we decide:

- whether it contains an object;
- the location of the object relative to the RoI.

In R-CNN, we start with a network pre-trained on ImageNet (VGG-16 is used in the original paper), and we use it to process *every RoI*, rescaling every one of them to the size of 224×224 .

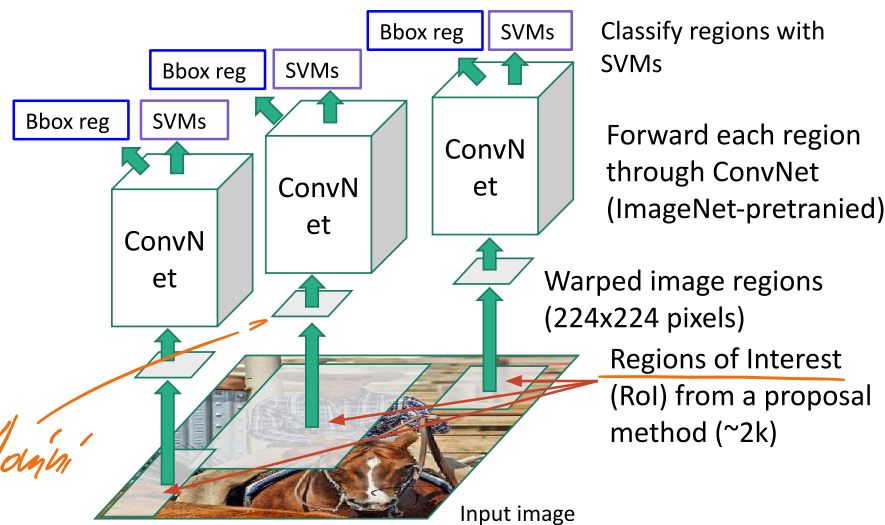
For every RoI, two sibling heads are added:

- *classification head* predicts either *background* or one of K object types ($K + 1$ in total),
- *bounding box regression head* predicts 4 bounding box parameters relative to RoI.

must train a by object to proposal specific CNN



Slide 48 of http://cs231n.stanford.edu/slides/2021/lecture_15.pdf.



Slide 54 of http://cs231n.stanford.edu/slides/2021/lecture_15.pdf.

R-CNN – Bounding Boxes

A bounding box is parametrized as follows. Let x_r, y_r, w_r, h_r be center coordinates and width and height of the RoI respectively, and let x, y, w, h be parameters of the bounding box. We represent the bounding box relative to the RoI as follows:

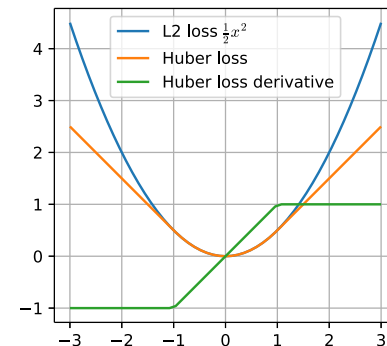
jakmile mám aktivaci fei $t_x = (x - x_r) / w_r, \quad t_y = (y - y_r) / h_r,$ *normalizace podle velikosti RoI*

exp, tak vždycky budu mít > 0. $t_w = \log(w / w_r), \quad t_h = \log(h / h_r).$ *zajisti, že šířka bude vždycky kladná.* *Uvažuj, že všechny RoI se vztahují na 224 x 224*

In Fast R-CNN, the smooth_{L_1} loss, or **Huber loss**, is employed for bounding box parameters:

- protože MSE je neomezená, může dát příliš velké gradienty

$$\text{smooth}_{L_1}(x) = \begin{cases} 0.5x^2 & \text{if } |x| < 1, \\ |x| - 0.5 & \text{otherwise.} \end{cases}$$

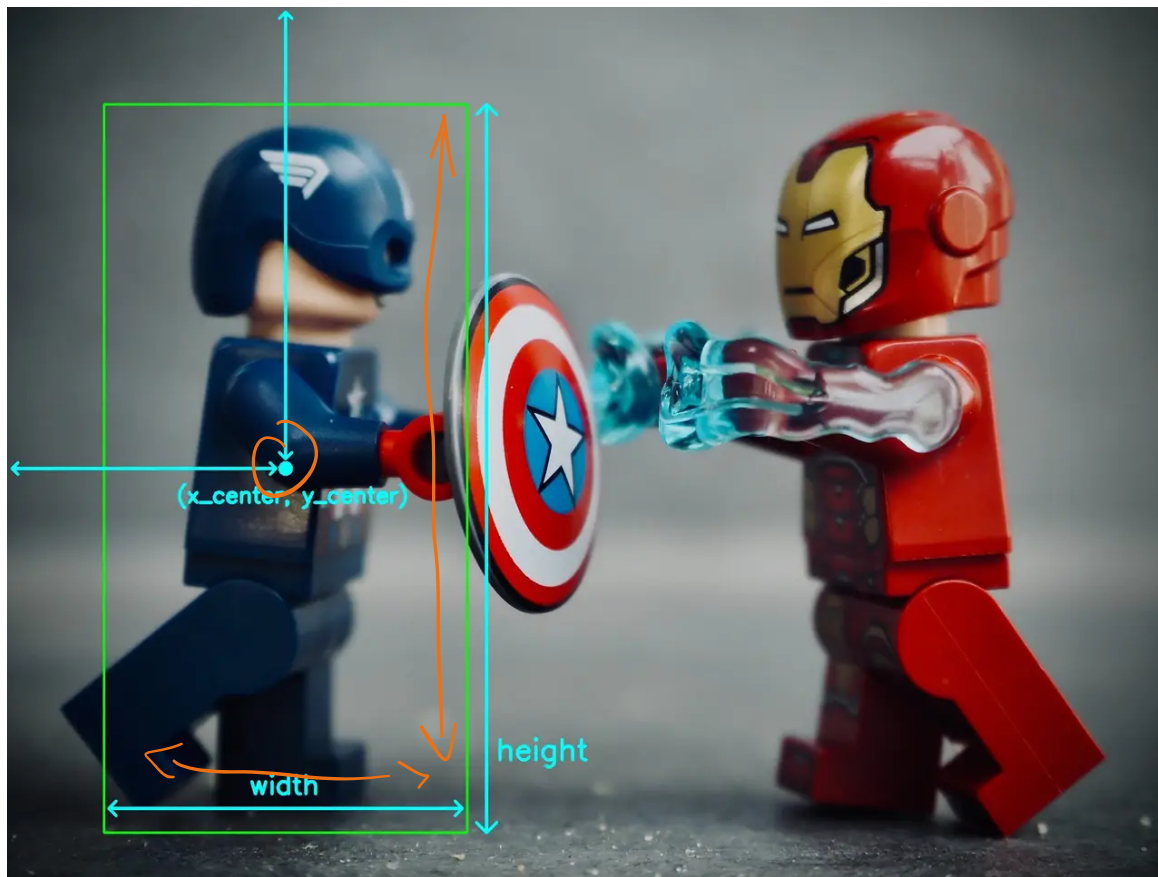


The complete loss is then ($\lambda = 1$ is used in the Fast R-CNN paper)

za klasifikaci $L(\hat{c}, \hat{t}, c, t) = L_{\text{cls}}(\hat{c}, c) + \lambda \cdot [c \geq 1] \cdot \sum_{i \in \{x, y, w, h\}} \text{smooth}_{L_1}(\hat{t}_i - t_i).$ *pokud to nebyl background*

pro vyučení

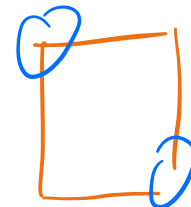
The described bounding box representation is usually called CXCXYWH:



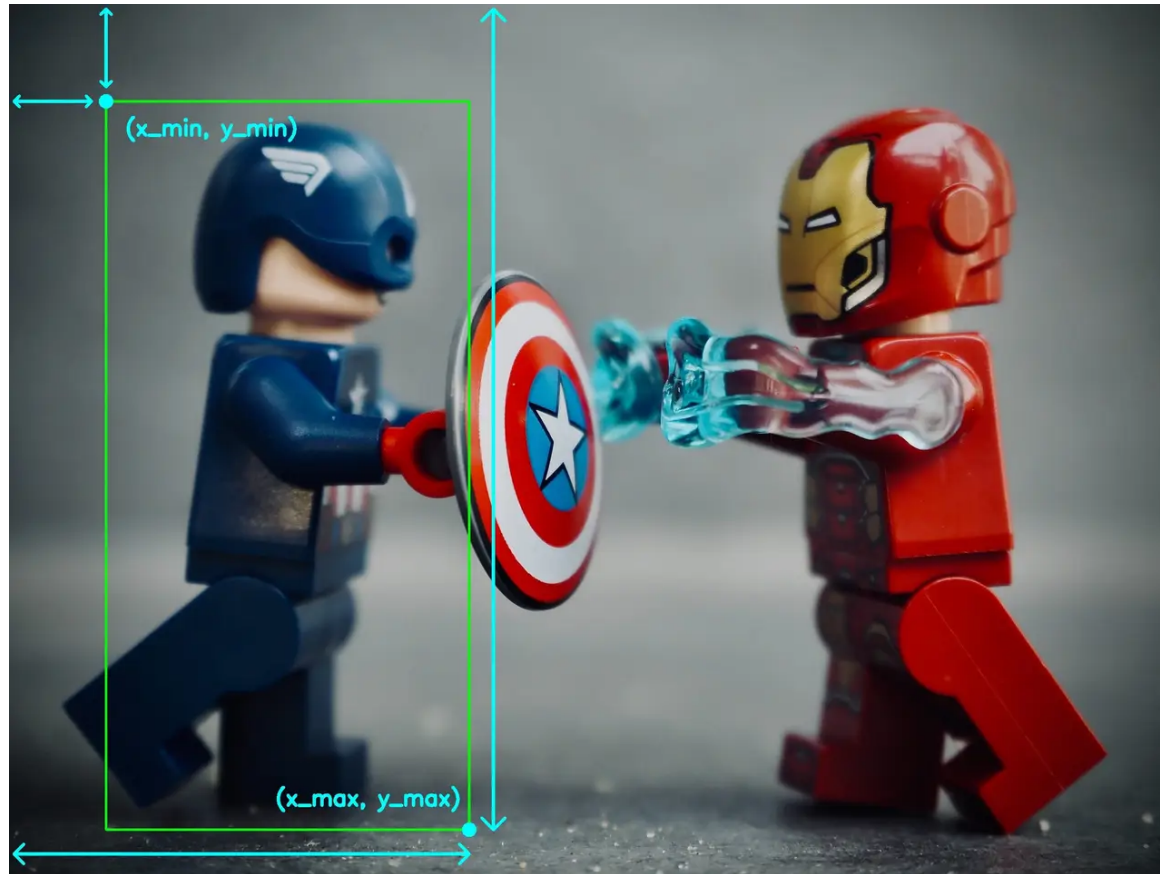
https://miro.medium.com/1*Z80D7vwD-3UwP16asY-k6A.jpeg

Ještě se používá

xyxy

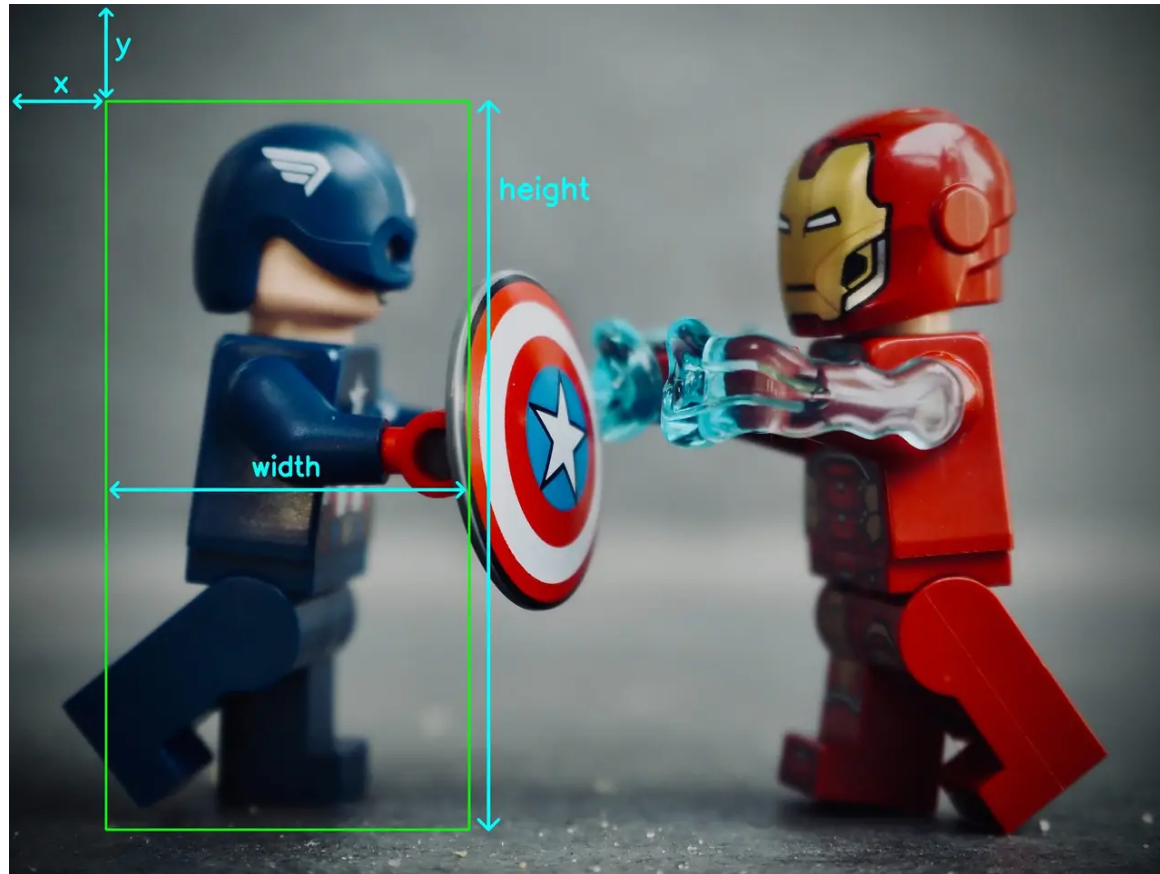


In the datasets, the bounding boxes are usually represented using XXYX format:



https://miro.medium.com/1*oZcZhzOWKb3kvBHPOHYfow.jpeg

Finally, you could also come across the XYWH format:

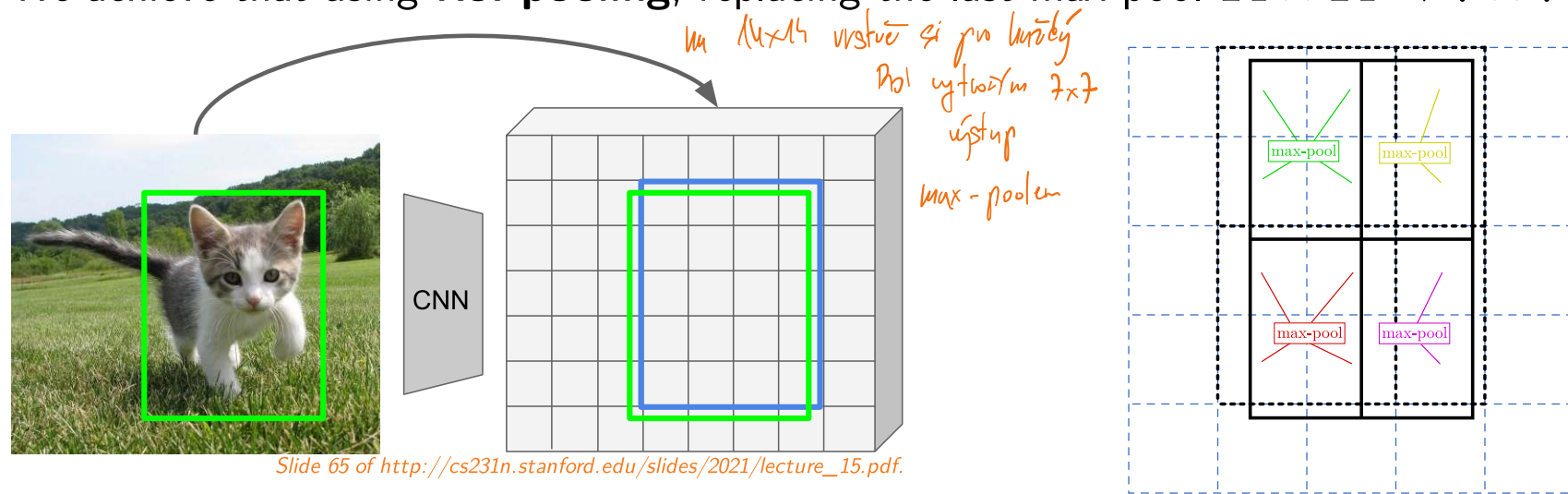


https://miro.medium.com/1*JLeFS2KIOzSTk6lUp10u2w.jpeg

Fast R-CNN Architecture

The R-CNN is slow, because it needs to process every RoI by the convolutional backbone. To speed it up, we might want to first process the whole image by the backbone and only then extract a fixed-size representation for every RoI.

We achieve that using **RoI pooling**, replacing the last max-pool $14 \times 14 \rightarrow 7 \times 7$ VGG layer.



During RoI pooling, we obtain a 7×7 RoI representation by first projecting the RoI to the 14×14 resolution and then computing each of the 7×7 values by **max-pooling** the corresponding “pixels” of the convolutional image features.

2 toho 16×16 obrázku místo \max -poolingu namapují ty jednotlivé RoI
na pixely z 16×16 a \max -pooling uděláme až na ty
jednotlivé segmenty pixelů, které odpovídají RoI.

↳ tzn. že pokud je segment malý, děláme pooling $1 \times 1 \rightarrow 1 \times 1$,
někdy ale zmenšujeme...

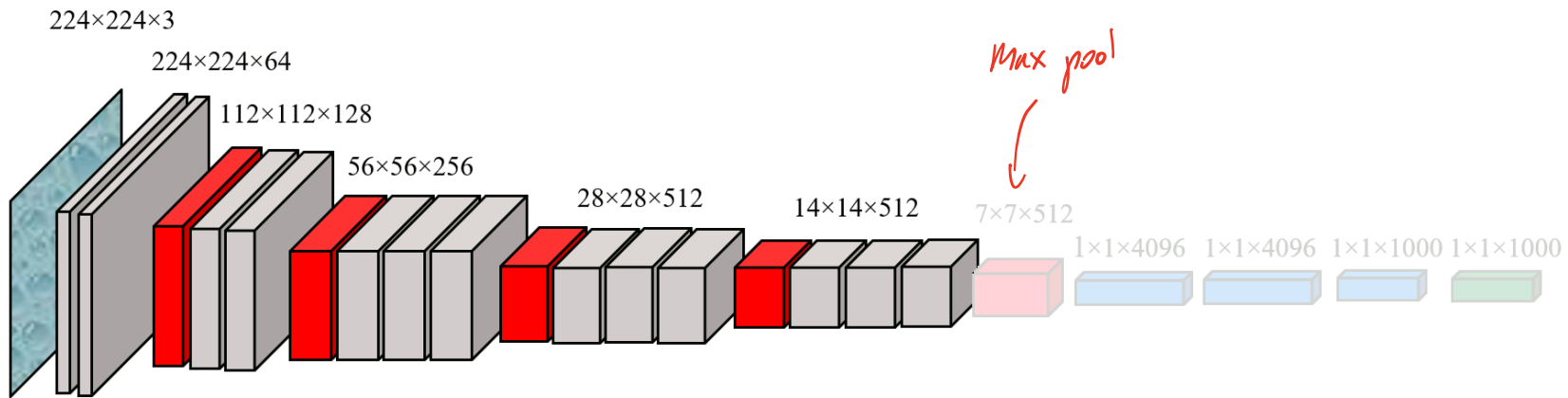
tabuře repr. různé velikosti RoI je stejně velké



RoI Representation

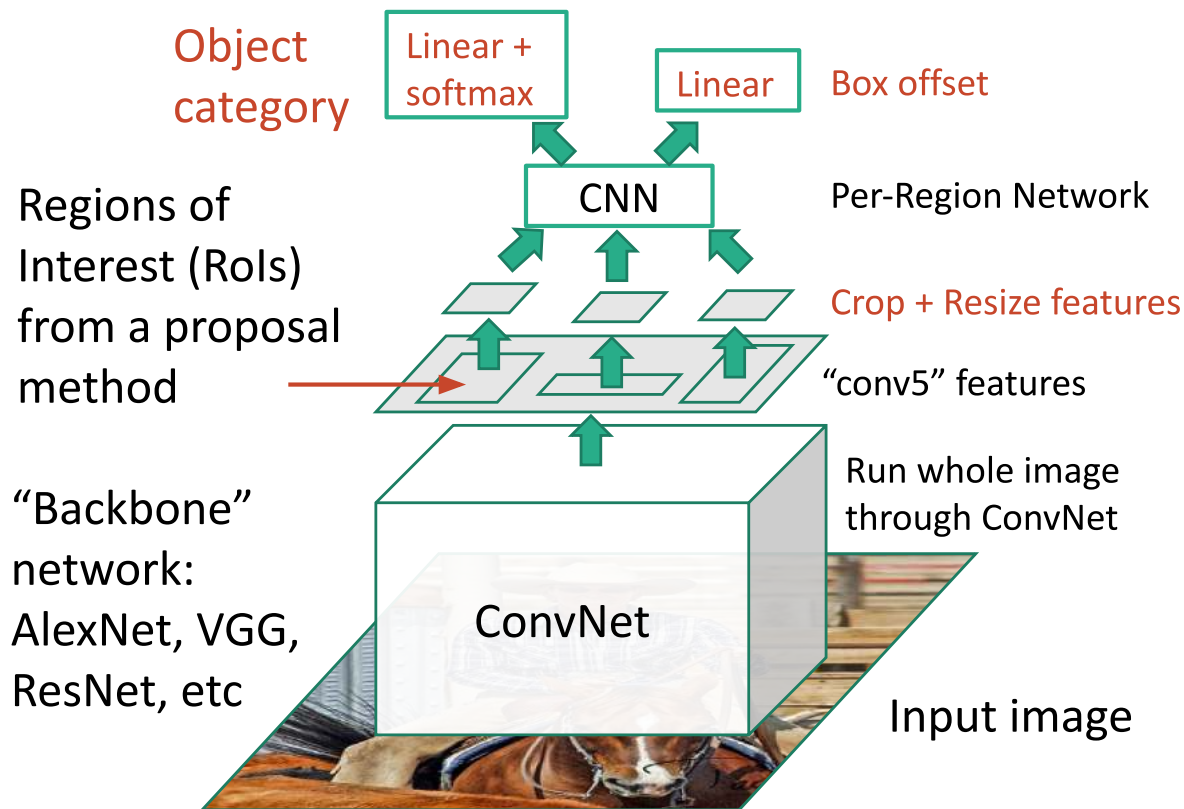


[https://commons.wikimedia.org/wiki/File:Tišnov,_Hajánky,_garážová_ozdoba_\(6597\).jpg](https://commons.wikimedia.org/wiki/File:Tišnov,_Hajánky,_garážová_ozdoba_(6597).jpg)

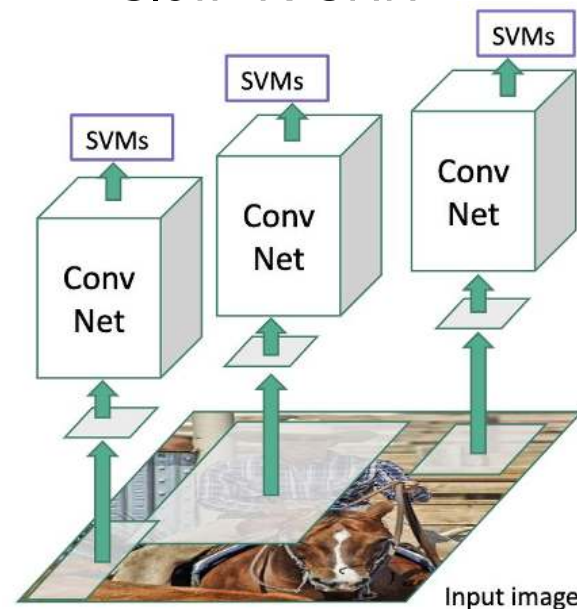


https://en.wikipedia.org/wiki/File:VGG_neural_network.png

Fast R-CNN



"Slow" R-CNN



Slide 61 of http://cs231n.stanford.edu/slides/2021/lecture_15.pdf.

Fast R-CNN Architecture

fast RoI přenesu 2 inputs do feature space

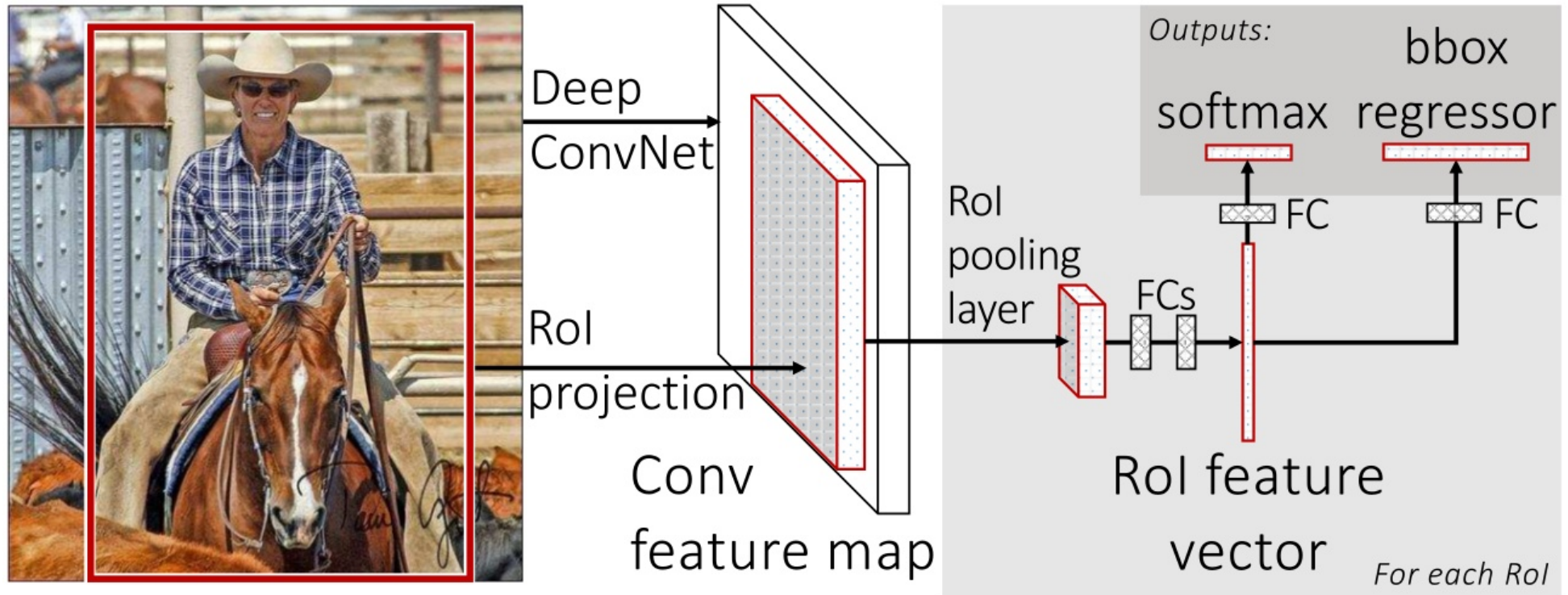


Figure 1 of "Fast R-CNN", <https://arxiv.org/abs/1504.08083>

Intersection over Union

For two bounding boxes (or two masks) the *intersection over union* (*IoU*) is a ratio of the intersection of the boxes (or masks) and the union of the boxes (or masks).

Choosing Rols for Training

During training, we use 2 images with 64 Rols each. The Rols are selected so that 25% have intersection over union (*IoU*) overlap with ground-truth boxes at least 0.5; the others are chosen to have the *IoU* in range $[0.1, 0.5]$, the so-called *hard examples*.

protože učit se úplně nic je zbytečné. → dostanu ještě třeba i 1000 RoIs

Running Inference

During inference, we utilize all RoIs, but a single object can be found in several of them. To choose the most salient prediction, we perform **non-maximum suppression** – we ignore predictions which have an overlap with a higher scoring prediction of the *same class*, where the overlap is computed using *IoU* (0.3 threshold is used in the paper). Higher scoring predictions is the ones with higher probability from the *classification head*.

tobto bylo obecně málo, ale jinak to mělo špatný výsledek

Average Precision

Evaluation is performed using *Average Precision* (AP or AP_{50}).

We assume all bounding boxes (or masks) produced by a system have **confidence values** which can be used to rank them. Then, for a single class, we take the boxes (or masks) in the order of the ranks and generate precision/recall curve, considering a bounding box correct if it has IoU at least 50% with any ground-truth box.

krivha idealna klasifikatsiya.

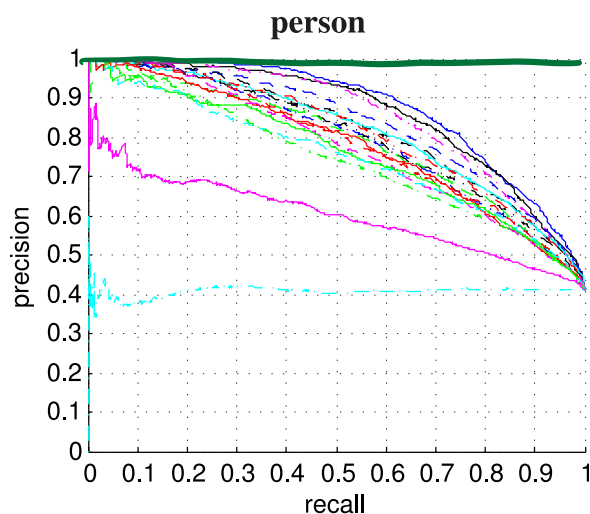


Figure 6 of "The PASCAL Visual Object Classes (VOC) Challenge",
http://homepages.inf.ed.ac.uk/ckiwi/postscript/ijcv_voc09.pdf

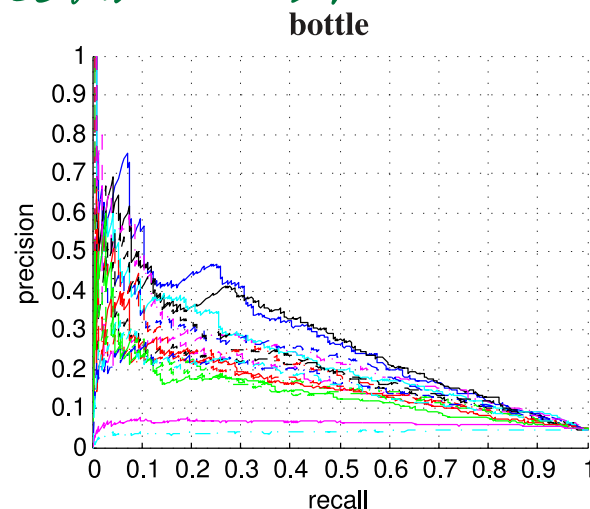
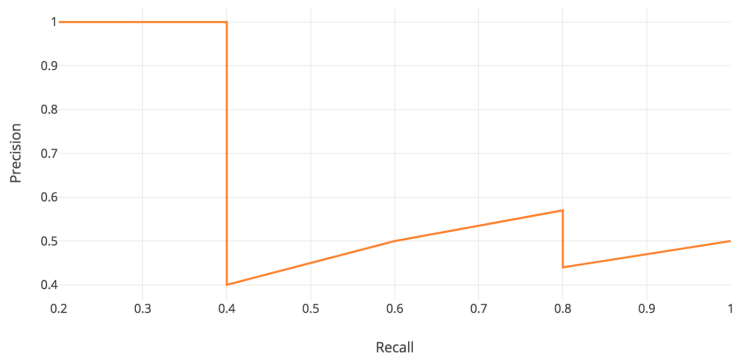


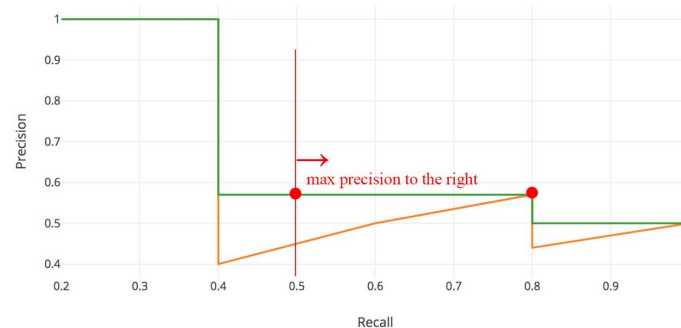
Figure 6 of "The PASCAL Visual Object Classes (VOC) Challenge",
http://homepages.inf.ed.ac.uk/ckiwi/postscript/ijcv_voc09.pdf

Object Detection Evaluation – Average Precision

The general idea of AP is to compute the area under the precision/recall curve.



https://miro.medium.com/max/1400/1*VenTq4lgxjmlpOXWdFb-jg.png



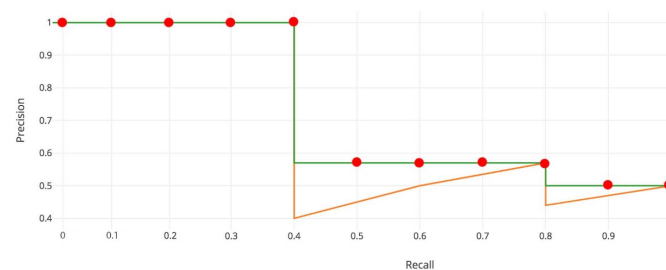
https://miro.medium.com/max/1400/1*pmSxeb4EfdGnzT6Xa68GEQ.jpeg

We start by interpolating the precision/recall curve, so that it is always nonincreasing.

Finally, the average precision for a single class is an average of precision at recall

0.0, 0.1, 0.2, ..., 1.0.

The final AP is a mean of average precision of all classes.



https://miro.medium.com/max/1400/1*naz02wO-XMywIwAdFzF-GA.jpeg

Object Detection Evaluation – Average Precision

For the COCO dataset, the AP is computed slightly differently. First, it is an average over 101 recall points $0.00, 0.01, 0.02, \dots, 1.00$.

In the original metric, IoU of 50% is enough to consider a prediction valid. We can generalize the definition to AP_t , where an object prediction is considered valid if IoU is at least $t\%$.

The main COCO metric, denoted just AP , is the mean of $AP_{50}, AP_{55}, AP_{60}, \dots, AP_{95}$.

| Metric | Description |
|-----------|--|
| AP | Mean of $AP_{50}, AP_{55}, AP_{60}, AP_{65}, \dots, AP_{95}$ |
| AP_{50} | AP at IoU 50% |
| AP_{75} | AP at IoU 75% |
| AP_S | AP for small objects: $area < 32^2$ |
| AP_M | AP for medium objects: $32^2 < area < 96^2$ |
| AP_L | AP for large objects: $96^2 < area$ |

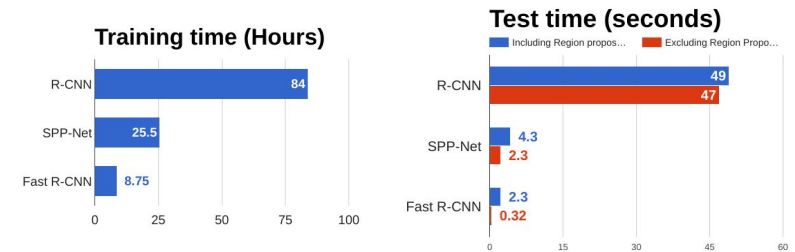
Even if Fast R-CNN is much faster than R-CNN, it can still be improved, considering that the most problematic and time consuming part is generating the Rols.

Časem se ukázalo, že by to šlo dělat rovnou jednodušeji, ale na to předtím ještě neměli výkon

Faster R-CNN extends Fast R-CNN by including a **region proposal network (RPN)**, whose goal is to generate the Rols automatically.

The regional proposal networks produces the so-called **region proposals**, which then play the role of Rols in the rest of the pipeline (i.e., the Fast R-CNN).

The region proposals are generated similarly to how predictions are generated in Fast R-CNN. We start with several **anchors** and from each anchor we generate either a single region proposal or nothing.



Slide 76 of http://cs231n.stanford.edu/slides/2021/lecture_15.pdf.

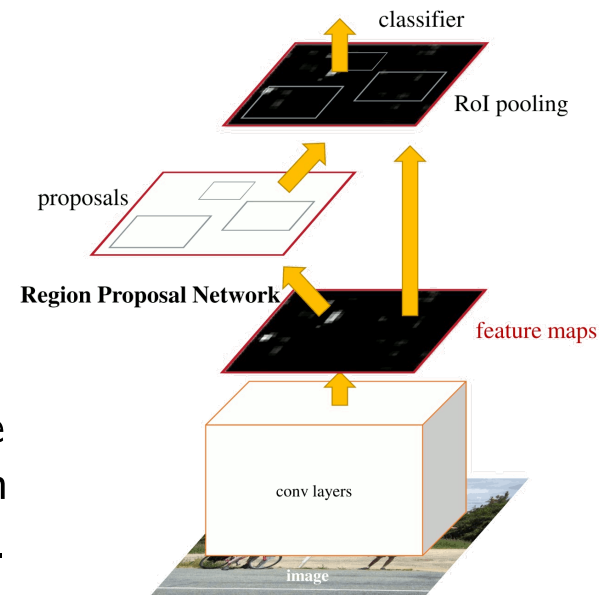
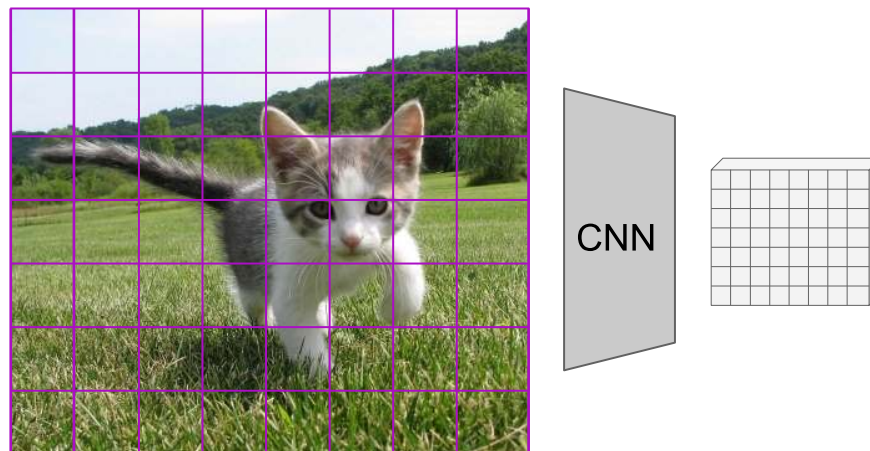


Figure 2 of "Faster R-CNN: Towards Real-Time Object Detection with Region Proposal Networks", <https://arxiv.org/abs/1506.01497>

If we consider the 14×14 VGG backbone output, each “pixel” corresponds to a region of size 16×16 in the original image.



Adapted from slide 65 of http://cs231n.stanford.edu/slides/2021/lecture_15.pdf.

We can therefore interpret each value in the 14×14 output as a representation of a part of the image *centered* in the corresponding image region, and try predicting a region proposal from **every one** of them.

We call the dense grid of image regions from which we are predicting the proposals the **anchors**. They have fixed size, and in practice we use *several* anchors per position.

For every anchor, we classify it in two classes (background, object) and also predict the region proposal bounding box relatively to the anchor, exactly as in (Fast) R-CNN.

We perform the classification and the bounding box regression by first running a 3×3 convolution followed by ReLU on the 14×14 VGG output, and then attaching the two heads. Assuming there are A anchors on every position:

- the classification head generates $2A$ outputs, performing softmax on every 2 of them;
- the regression head generates $4A$ region proposal coordinates.

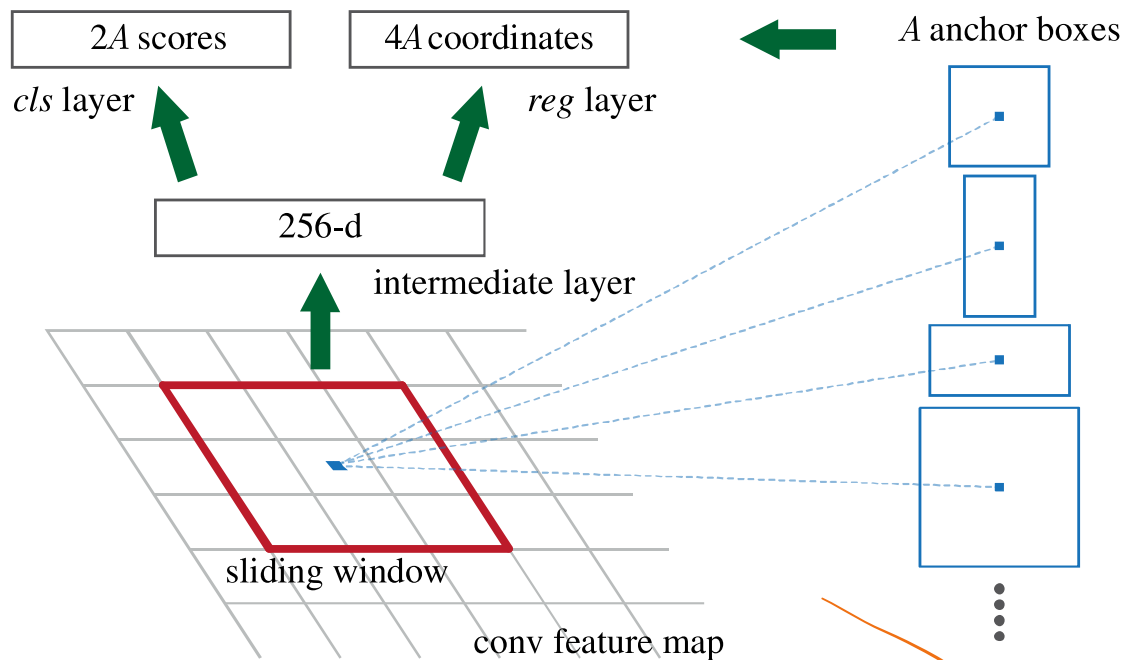


Figure 3 of "Faster R-CNN: Towards Real-Time Object Detection with Region Proposal Networks", <https://arxiv.org/abs/1506.01497>

The authors consider 3 scales ($128^2, 256^2, 512^2$) and 3 aspect ratios ($1 : 1, 1 : 2, 2 : 1$).

tohle je stejný klam jako u fast R-CNN



During training, we generate

- positive training examples for every anchor that has the highest IoU with a ground-truth box;
- furthermore, a positive example is also any anchor with IoU at least 0.7 for any ground-truth box;
- negative training examples for every anchor that has IoU at most 0.3 with all ground-truth boxes;
- the positive and negative examples are generated with a ratio *up to* 1:1 (less, if there are not enough positive examples; each minibatch consists of a single image and 256 anchors).

During inference, we consider all predicted non-background regions, run non-maximum suppression on them using a 0.7 IoU threshold, and then take N top-scored regions (i.e., the ones with the highest probability from the classification head) – the paper uses 300 proposals, compared to 2000 in the Fast R-CNN.

Table 3: Detection results on **PASCAL VOC 2007 test set**. The detector is Fast R-CNN and VGG-16. Training data: “07”: VOC 2007 trainval, “07+12”: union set of VOC 2007 trainval and VOC 2012 trainval. For RPN, the train-time proposals for Fast R-CNN are 2000. [†]: this number was reported in [2]; using the repository provided by this paper, this result is higher (68.1).

| method | # proposals | data | mAP (%) |
|-------------------|-------------|------------|-------------------|
| SS | 2000 | 07 | 66.9 [†] |
| SS | 2000 | 07+12 | 70.0 |
| RPN+VGG, unshared | 300 | 07 | 68.5 |
| RPN+VGG, shared | 300 | 07 | 69.9 |
| RPN+VGG, shared | 300 | 07+12 | 73.2 |
| RPN+VGG, shared | 300 | COCO+07+12 | 78.8 |

Table 4: Detection results on **PASCAL VOC 2012 test set**. The detector is Fast R-CNN and VGG-16. Training data: “07”: VOC 2007 trainval, “07++12”: union set of VOC 2007 trainval+test and VOC 2012 trainval. For RPN, the train-time proposals for Fast R-CNN are 2000. [†]: <http://host.robots.ox.ac.uk:8080/anonymous/HZJTQA.html>. [‡]: <http://host.robots.ox.ac.uk:8080/anonymous/YNPLXB.html>. [§]: <http://host.robots.ox.ac.uk:8080/anonymous/XEDH10.html>.

| method | # proposals | data | mAP (%) |
|------------------------------|-------------|-------------|-------------|
| SS | 2000 | 12 | 65.7 |
| SS | 2000 | 07++12 | 68.4 |
| RPN+VGG, shared [†] | 300 | 12 | 67.0 |
| RPN+VGG, shared [‡] | 300 | 07++12 | 70.4 |
| RPN+VGG, shared [§] | 300 | COCO+07++12 | 75.9 |

Tables 3 and 4 of “Faster R-CNN: Towards Real-Time Object Detection with Region Proposal Networks”, <https://arxiv.org/abs/1506.01497>

The Faster R-CNN is a so-called **two-stage** detector, where the regions are refined twice – once in the region proposal network, and then in the final bounding box regressor.

Several **single-stage** detector architectures have been proposed, mainly because they are faster and smaller, but until circa 2017 the two-stage detectors achieved better results.

Straightforward extension of Faster R-CNN able to produce image segmentation (i.e., masks for every object).



Figure 2 of "Mask R-CNN", <https://arxiv.org/abs/1703.06870>

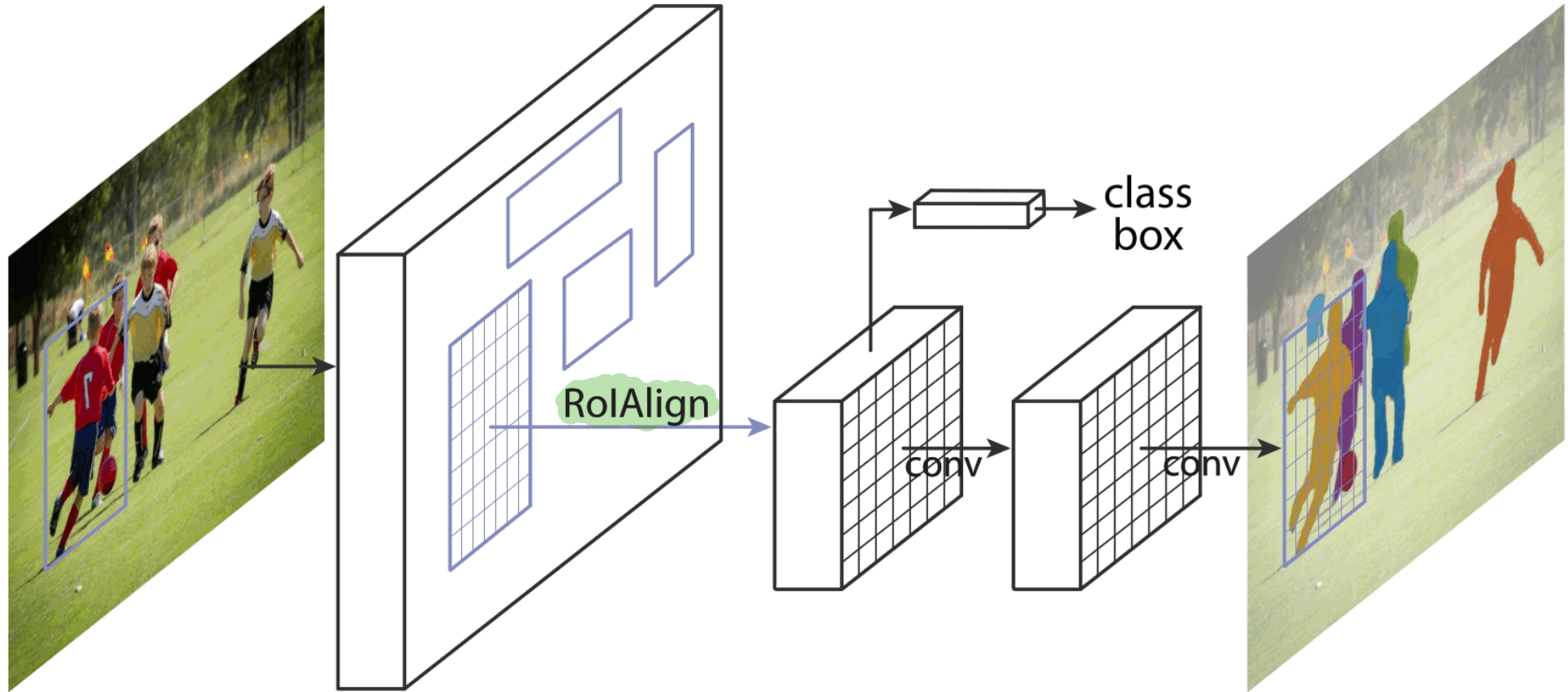


Figure 1 of "Mask R-CNN", <https://arxiv.org/abs/1703.06870>

More precise alignment is required for the RoI in order to predict the masks. Instead of quantization and max-pooling in RoI pooling, **RoIAlign** uses bilinear interpolation of features at four regularly sampled locations in each RoI bin and averages them.

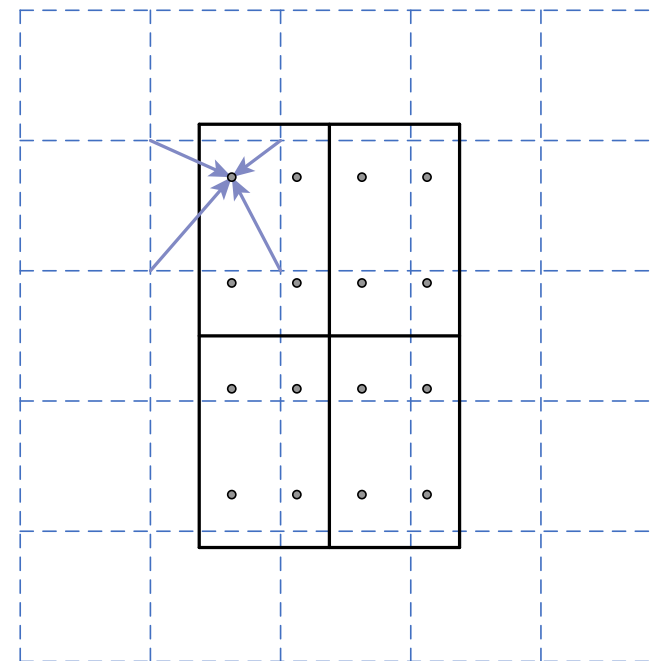
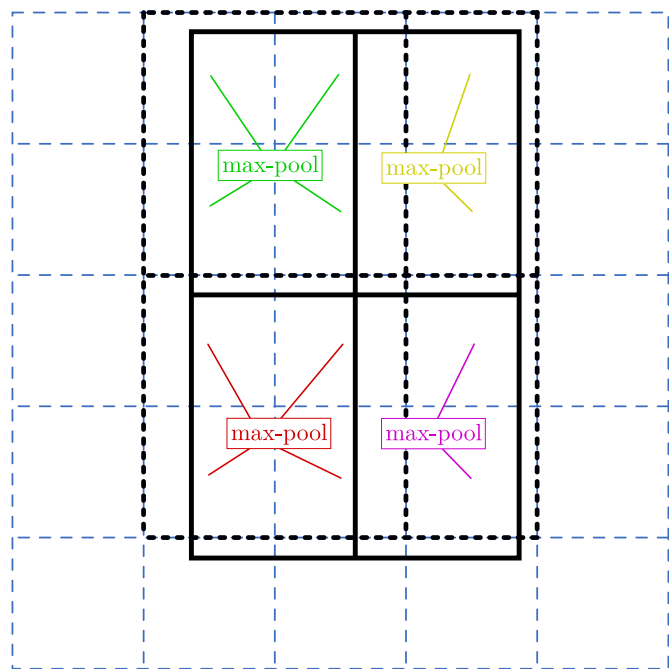


Figure 3 of "Mask R-CNN", <https://arxiv.org/abs/1703.06870>

TorchVision provides `torchvision.ops.roi_align` and `torchvision.ops.roi_pool`.

Masks are predicted in a third branch of the object detector.

- Higher resolution of the mask is usually needed (at least 14×14 , or even more).
- The masks are predicted for each class separately.
- The masks are predicted using convolutions instead of fully connected layers (the upscaling convolutions are 2×2 with stride 2).

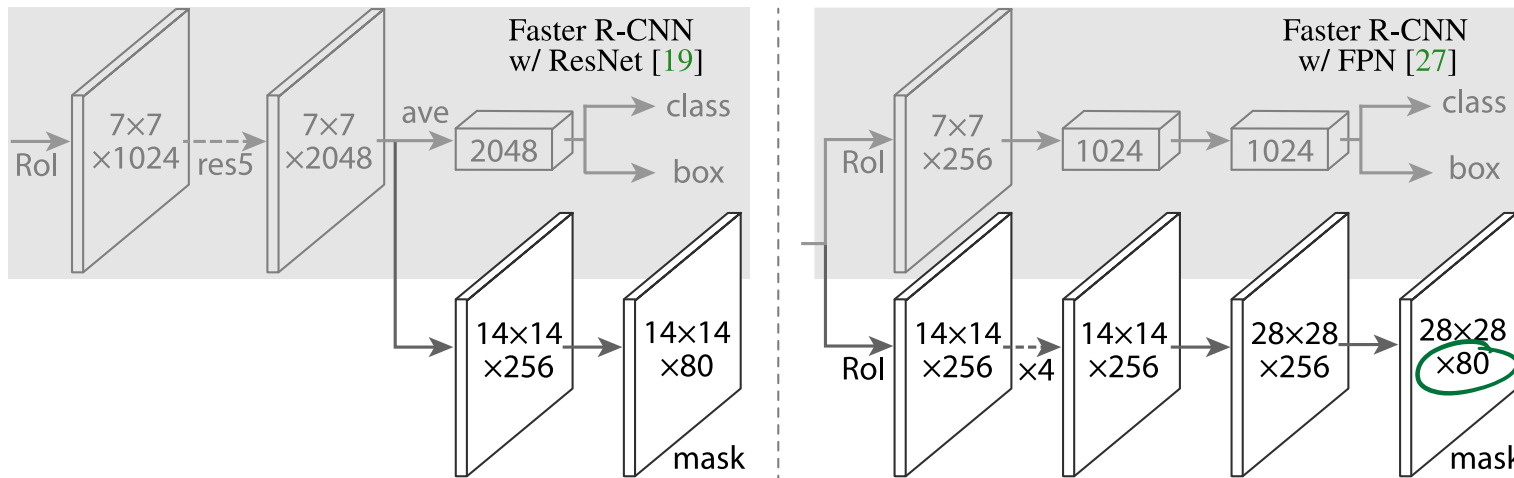


Figure 4 of "Mask R-CNN", <https://arxiv.org/abs/1703.06870>

Improvements from Nov 2021: all convs (except for the output layer) are followed by BN, the *class&bbox* head uses 4 convs instead of 2 MLPs, RPN contains two convs instead of one.

| <i>net-depth-features</i> | AP | AP ₅₀ | AP ₇₅ |
|---------------------------|-------------|------------------|------------------|
| ResNet-50-C4 | 30.3 | 51.2 | 31.5 |
| ResNet-101-C4 | 32.7 | 54.2 | 34.3 |
| ResNet-50-FPN | 33.6 | 55.2 | 35.3 |
| ResNet-101-FPN | 35.4 | 57.3 | 37.5 |
| ResNeXt-101-FPN | 36.7 | 59.5 | 38.9 |

(a) **Backbone Architecture:** Better backbones bring expected gains: deeper networks do better, FPN outperforms C4 features, and ResNeXt improves on ResNet.

| | AP | AP ₅₀ | AP ₇₅ |
|----------------|-------------|------------------|------------------|
| <i>softmax</i> | 24.8 | 44.1 | 25.1 |
| <i>sigmoid</i> | 30.3 | 51.2 | 31.5 |
| | +5.5 | +7.1 | +6.4 |

(b) **Multinomial vs. Independent Masks** (ResNet-50-C4): *Decoupling* via per-class binary masks (sigmoid) gives large gains over multinomial masks (softmax).

| | align? | bilinear? | agg. | AP | AP ₅₀ | AP ₇₅ |
|---------------------|--------|-----------|------|-------------|------------------|------------------|
| <i>RoIPool</i> [12] | | | max | 26.9 | 48.8 | 26.4 |
| <i>RoIWarp</i> [10] | | ✓ | max | 27.2 | 49.2 | 27.1 |
| | | ✓ | ave | 27.1 | 48.9 | 27.1 |
| <i>RoIAlign</i> | ✓ | ✓ | max | 30.2 | 51.0 | 31.8 |
| | ✓ | ✓ | ave | 30.3 | 51.2 | 31.5 |

(c) **RoIAlign** (ResNet-50-C4): Mask results with various RoI layers. Our RoIAlign layer improves AP by ~3 points and AP₇₅ by ~5 points. Using proper alignment is the only factor that contributes to the large gap between RoI layers.

| | AP | AP ₅₀ | AP ₇₅ | AP ^{bb} | AP ^{bb} ₅₀ | AP ^{bb} ₇₅ |
|-----------------|-------------|------------------|------------------|------------------|--------------------------------|--------------------------------|
| <i>RoIPool</i> | 23.6 | 46.5 | 21.6 | 28.2 | 52.7 | 26.9 |
| <i>RoIAlign</i> | 30.9 | 51.8 | 32.1 | 34.0 | 55.3 | 36.4 |
| | +7.3 | + 5.3 | +10.5 | +5.8 | +2.6 | +9.5 |

(d) **RoIAlign** (ResNet-50-C5, *stride* 32): Mask-level and box-level AP using *large-stride* features. Misalignments are more severe than with stride-16 features (Table 2c), resulting in big accuracy gaps.

| | mask branch | AP | AP ₅₀ | AP ₇₅ |
|-----|---------------------------------------|-------------|------------------|------------------|
| MLP | fc: 1024→1024→80·28 ² | 31.5 | 53.7 | 32.8 |
| MLP | fc: 1024→1024→1024→80·28 ² | 31.5 | 54.0 | 32.6 |
| FCN | conv: 256→256→256→256→256→80 | 33.6 | 55.2 | 35.3 |

(e) **Mask Branch** (ResNet-50-FPN): Fully convolutional networks (FCN) vs. multi-layer perceptrons (MLP, fully-connected) for mask prediction. FCNs improve results as they take advantage of explicitly encoding spatial layout.

Table 2. **Ablations.** We train on trainval35k, test on minival, and report *mask* AP unless otherwise noted.

Table 2 of "Mask R-CNN", <https://arxiv.org/abs/1703.06870>



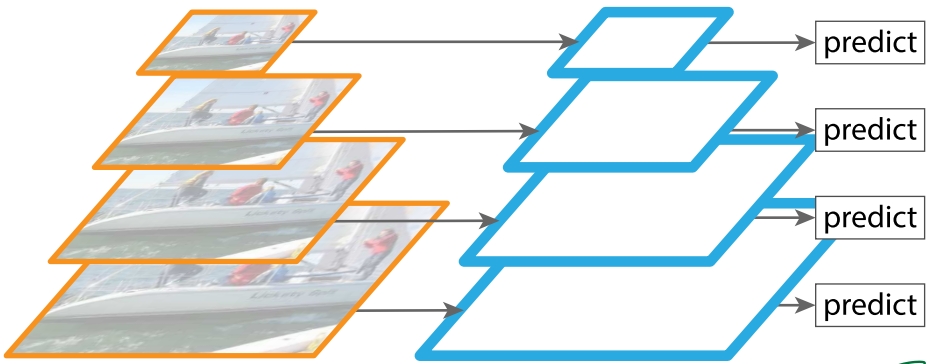
Figure 7 of "Mask R-CNN", <https://arxiv.org/abs/1703.06870>

- Testing applicability of Mask R-CNN architecture.
- Keypoints (e.g., left shoulder, right elbow, ...) are detected as independent one-hot masks of size 56×56 with softmax output function.

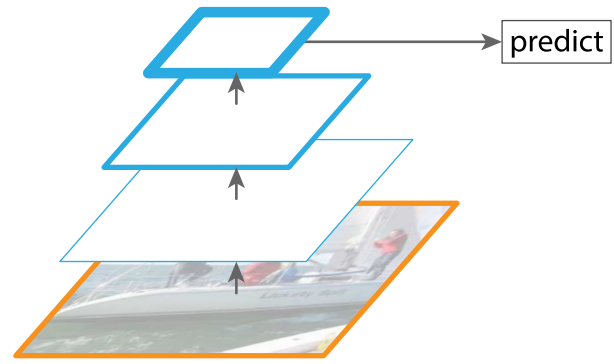
| | AP^{kp} | AP_{50}^{kp} | AP_{75}^{kp} | AP_M^{kp} | AP_L^{kp} |
|--|-------------|----------------|----------------|-------------|-------------|
| CMU-Pose+++ [6] | 61.8 | 84.9 | 67.5 | 57.1 | 68.2 |
| G-RMI [32] [†] | 62.4 | 84.0 | 68.5 | 59.1 | 68.1 |
| Mask R-CNN, keypoint-only | 62.7 | 87.0 | 68.4 | 57.4 | 71.1 |
| Mask R-CNN, keypoint & mask | 63.1 | 87.3 | 68.7 | 57.8 | 71.4 |

Table 4 of "Mask R-CNN", <https://arxiv.org/abs/1703.06870>

Feature Pyramid Networks



(a) Featurized image pyramid

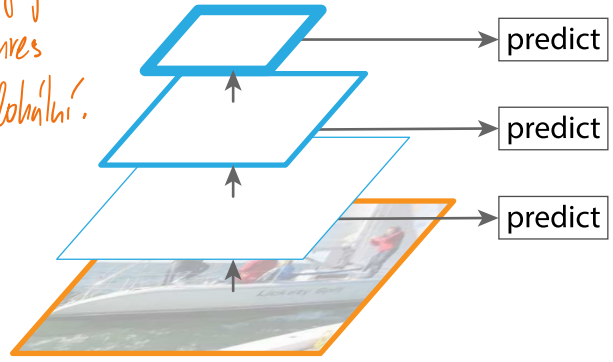


(b) Single feature map

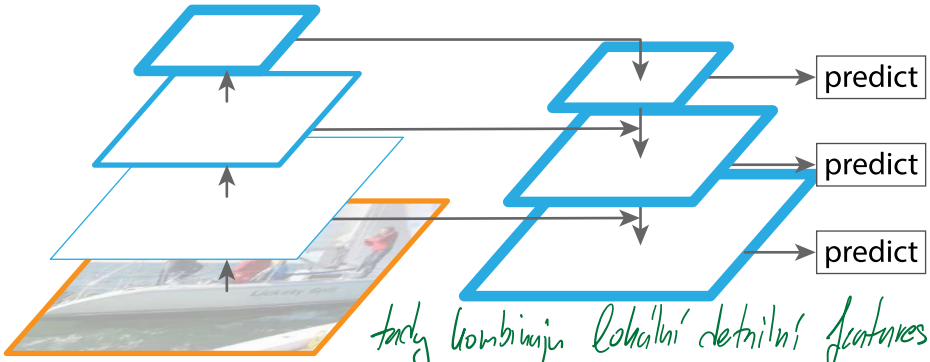
- takhle nefunguje dobře
protože features
jsou moc lokální.

- kvůli se zde ztrácí

takhle jsme dělali



(c) Pyramidal feature hierarchy



(d) Feature Pyramid Network

tedy kombinují lokální detailní features s globálními abstrakcemi

Figure 1 of "Feature Pyramid Networks for Object Detection", <https://arxiv.org/abs/1612.03144>

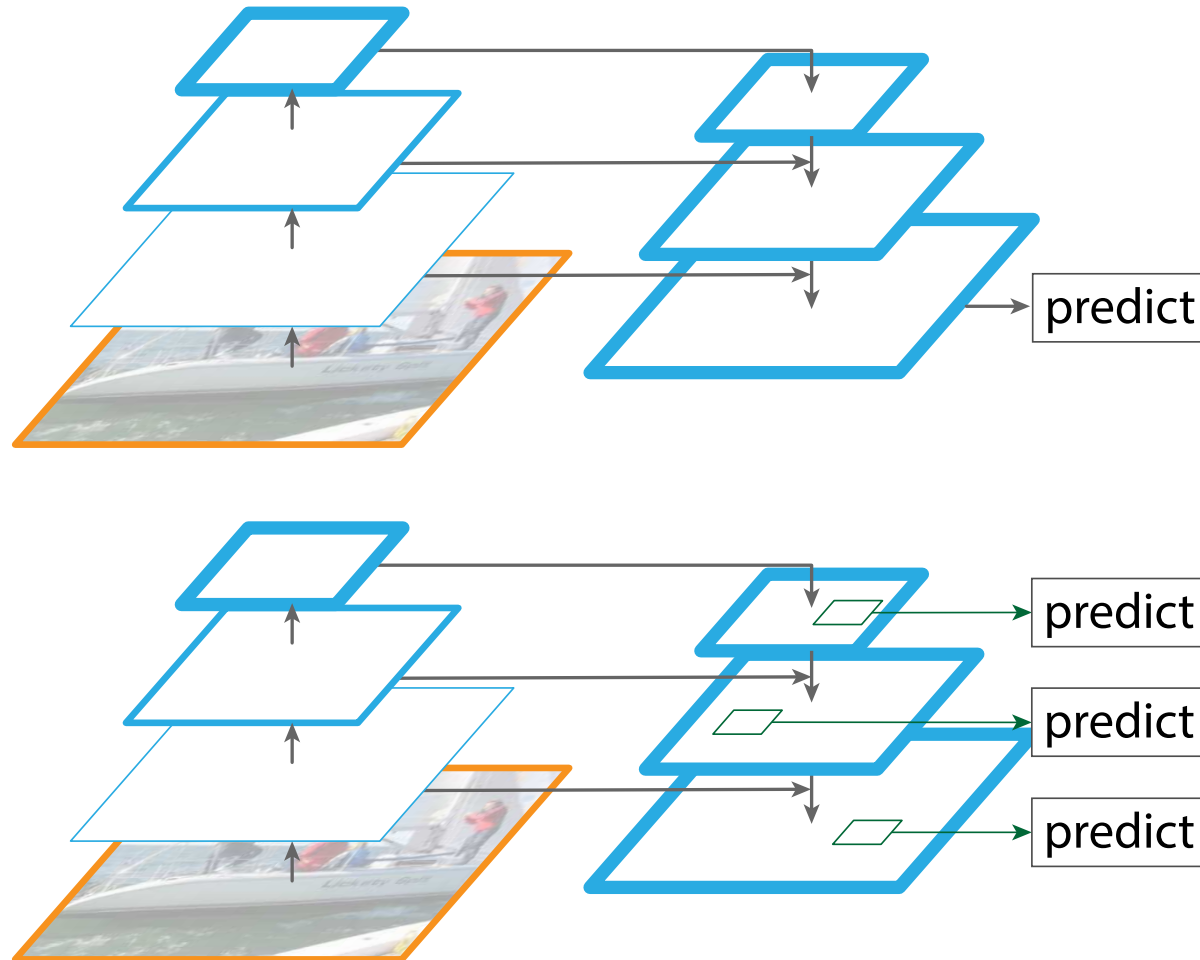


Figure 2 of "Feature Pyramid Networks for Object Detection", <https://arxiv.org/abs/1612.03144>

Feature Pyramid Networks

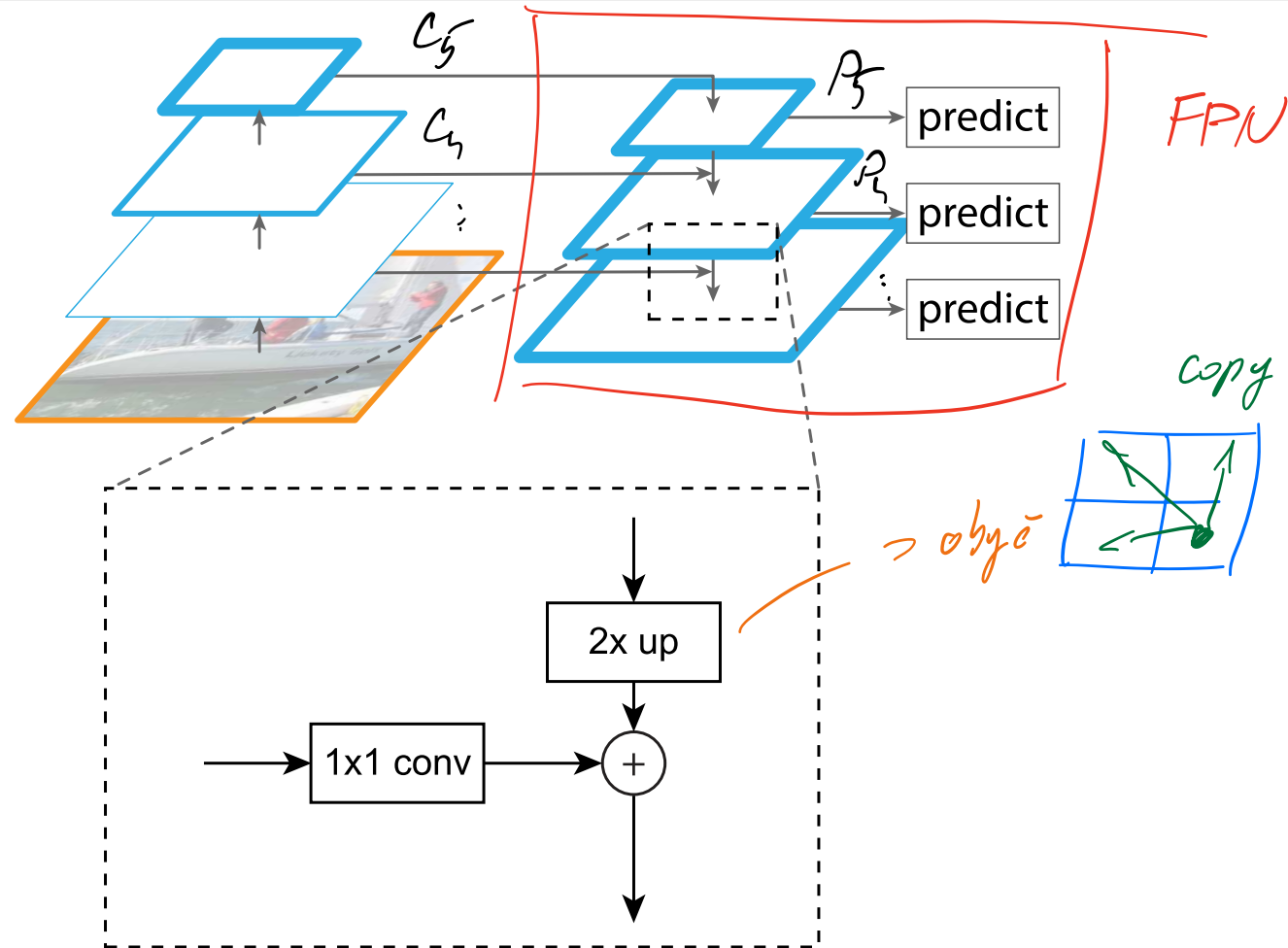


Figure 3 of "Feature Pyramid Networks for Object Detection", <https://arxiv.org/abs/1612.03144>

Feature Pyramid Networks

We employ FPN as a backbone in Faster R-CNN.

Assuming ResNet-like network with 224×224 input, we denote C_2, C_3, \dots, C_5 the image features of the last convolutional layer of size $56 \times 56, 28 \times 28, \dots, 7 \times 7$ (i.e., C_i indicates a downscaling of 2^i). The FPN representations incorporating the smaller resolution features are denoted as P_2, \dots, P_5 , each consisting of 256 channels; the classification heads are shared.

In both the RPN and the Fast R-CNN, authors utilize the P_2, \dots, P_5 representations, considering single-size anchors for every P_i (of size $32^2, 64^2, 128^2, 256^2$, respectively).

However, three aspect ratios ($1 : 1, 1 : 2, 2 : 1$) are still used. *↳ už nepotrebný veľkosť anchors*

| method | backbone | competition | image pyramid | test-dev | | | | | test-std | | | | |
|----------------------------------|------------|-------------|---------------|-------------|-------------|-----------------|-----------------|-----------------|-------------|-------------|-----------------|-----------------|-----------------|
| | | | | AP@.5 | AP | AP _s | AP _m | AP _l | AP@.5 | AP | AP _s | AP _m | AP _l |
| ours, Faster R-CNN on FPN | ResNet-101 | - | | 59.1 | 36.2 | 18.2 | 39.0 | 48.2 | 58.5 | 35.8 | 17.5 | 38.7 | 47.8 |

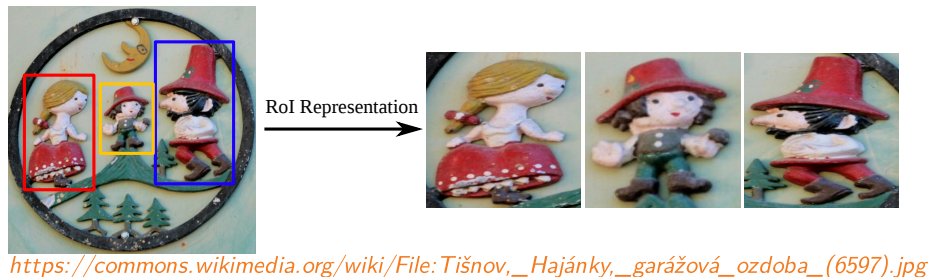
Competition-winning **single-model** results follow:

| | | | | | | | | | | | | | |
|---------------------------------|----------------------------------|------|---|------|------|------|------|-------------|------|------|------|------|-------------|
| G-RMI [†] | Inception-ResNet | 2016 | | - | 34.7 | - | - | - | - | - | - | - | - |
| AttractionNet [‡] [10] | VGG16 + Wide ResNet [§] | 2016 | ✓ | 53.4 | 35.7 | 15.6 | 38.0 | 52.7 | 52.9 | 35.3 | 14.7 | 37.6 | 51.9 |
| Faster R-CNN +++ [16] | ResNet-101 | 2015 | ✓ | 55.7 | 34.9 | 15.6 | 38.7 | 50.9 | - | - | - | - | - |
| Multipath [40] (on minival) | VGG-16 | 2015 | | 49.6 | 31.5 | - | - | - | - | - | - | - | - |
| ION [‡] [2] | VGG-16 | 2015 | | 53.4 | 31.2 | 12.8 | 32.9 | 45.2 | 52.9 | 30.7 | 11.8 | 32.8 | 44.8 |

Table 4 of "Feature Pyramid Networks for Object Detection", <https://arxiv.org/abs/1612.03144>

Focal Loss

For single-stage object detection architectures, *class imbalance* has been identified as the main issue preventing obtaining performance comparable to two-stage detectors. In a single-stage detector, there can be tens of thousands of anchors, with only dozens of useful training examples.



Cross-entropy loss is computed as

$$\mathcal{L}_{\text{cross-entropy}} = -\log p_{\text{model}}(y|x).$$

Focal-loss (loss focused on hard examples) is proposed as

$$\mathcal{L}_{\text{focal-loss}} = \underbrace{-(1 - p_{\text{model}}(y|x))^\gamma}_{\text{NLL}} \cdot \log p_{\text{model}}(y|x).$$

Handwritten note: 1 - probability of correct class

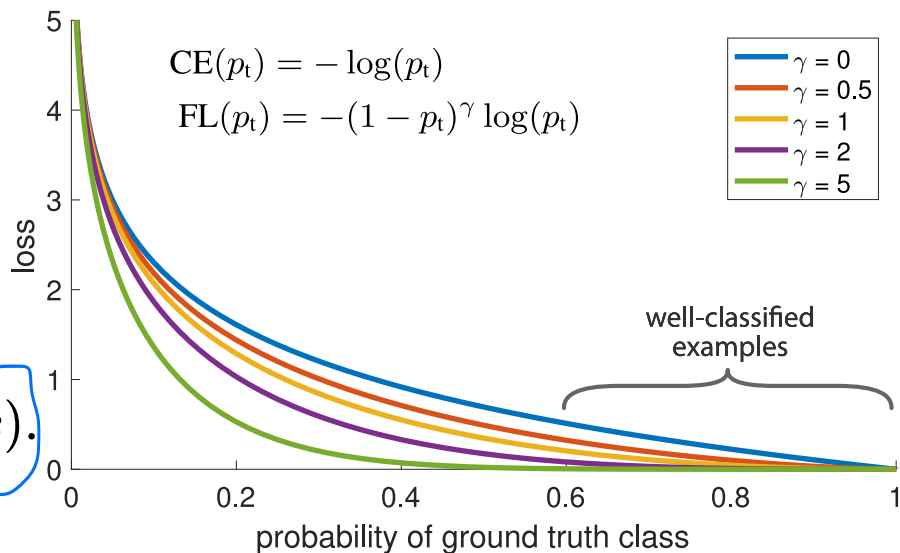


Figure 1 of "Focal Loss for Dense Object Detection", <https://arxiv.org/abs/1708.02002>

Focal Loss

For $\gamma = 0$, focal loss is equal to cross-entropy loss.

Authors reported that $\gamma = 2$ worked best for them for training a single-stage detector.

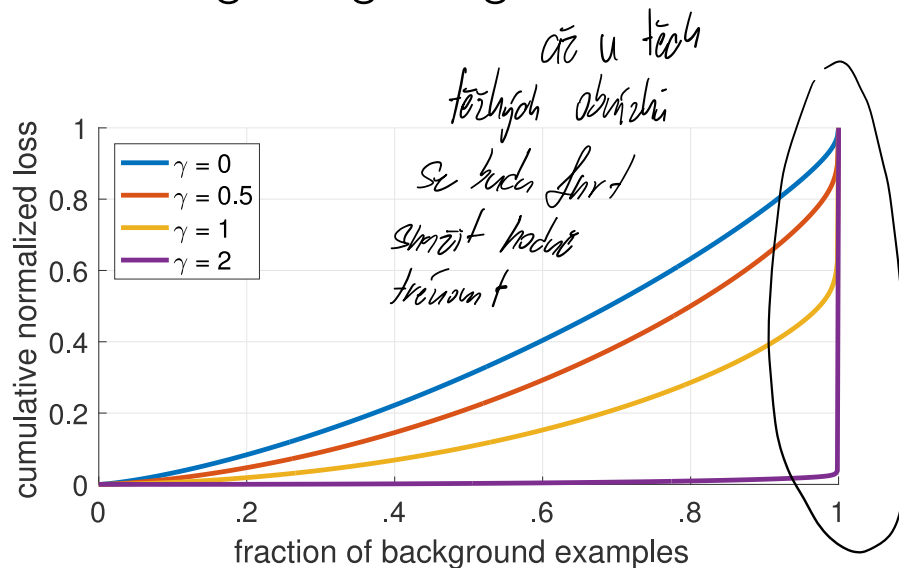
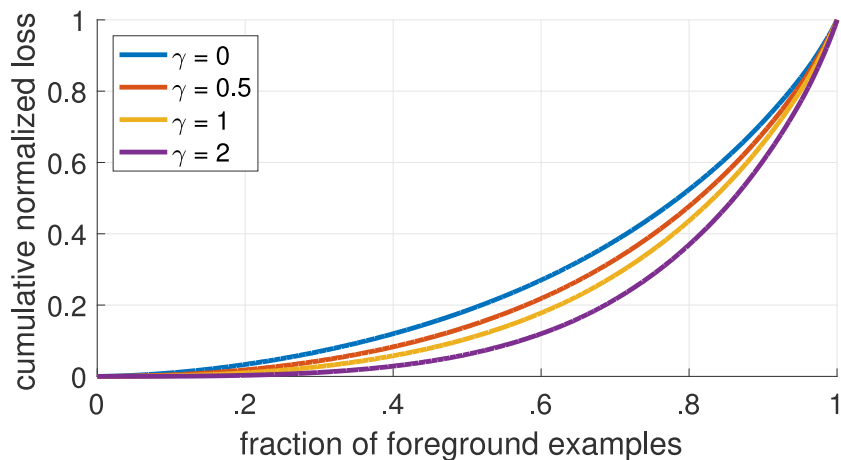


Figure 4. Cumulative distribution functions of the normalized loss for positive and negative samples for different values of γ for a *converged* model. The effect of changing γ on the distribution of the loss for positive examples is minor. For negatives, however, increasing γ heavily concentrates the loss on hard examples, focusing nearly all attention away from easy negatives.

Figure 4 of "Focal Loss for Dense Object Detection", <https://arxiv.org/abs/1708.02002>

Focal loss is connected to another solution to class imbalance – we might introduce weighting factor $\alpha \in (0, 1)$ for one class and $1 - \alpha$ for the other class, arriving at

$$-\alpha_y \cdot \log p_{\text{model}}(y|x).$$

The weight α might be set to the inverse class frequency or treated as a hyperparameter.

Even if weighting focuses more on low-frequent class, it does not distinguish between easy and hard examples, contrary to focal loss.

In practice, the focal loss is usually used together with class weighting:

$$-\alpha_y \cdot (1 - p_{\text{model}}(y|x))^\gamma \cdot \log p_{\text{model}}(y|x).$$

staticky

dynamicky

For example, authors report that $\alpha = 0.25$ (weight of the rare class) works best with $\gamma = 2$.

Toto je nejlepší inženýrský přístup

RetinaNet is a single-stage detector, using feature pyramid network architecture. Built on top of ResNet architecture, the feature pyramid contains levels P_3 through P_7 , with each P_l having 256 channels and resolution 2^l times lower than the input. On each pyramid level P_l , we consider 9 anchors for every position, with 3 different aspect ratios (1, 1 : 2, 2 : 1) and with 3 different sizes ($\{2^0, 2^{1/3}, 2^{2/3}\} \cdot 4 \cdot 2^l$)². *→ dřívešobly už nemají singel, protože to je další úroveň*

Note that ResNet provides only C_3 to C_5 features. C_6 is computed using a 3×3 convolution with stride 2 on C_5 , and C_7 is obtained by applying ReLU followed by another 3×3 stride-2 convolution. The C_6 and C_7 are included to improve large object detection.

C_5 furt mají docela malé rozlišení, jsou hodně globální, obecný

tyhle si určujeme sami

RetinaNet – Architecture

The classification head and the boundary regression heads are fully convolutional and do not share parameters (but classification heads are shared across levels, and so are the boundary regression heads), generating *anchors · classes* sigmoids and *anchors* bounding boxes per position.

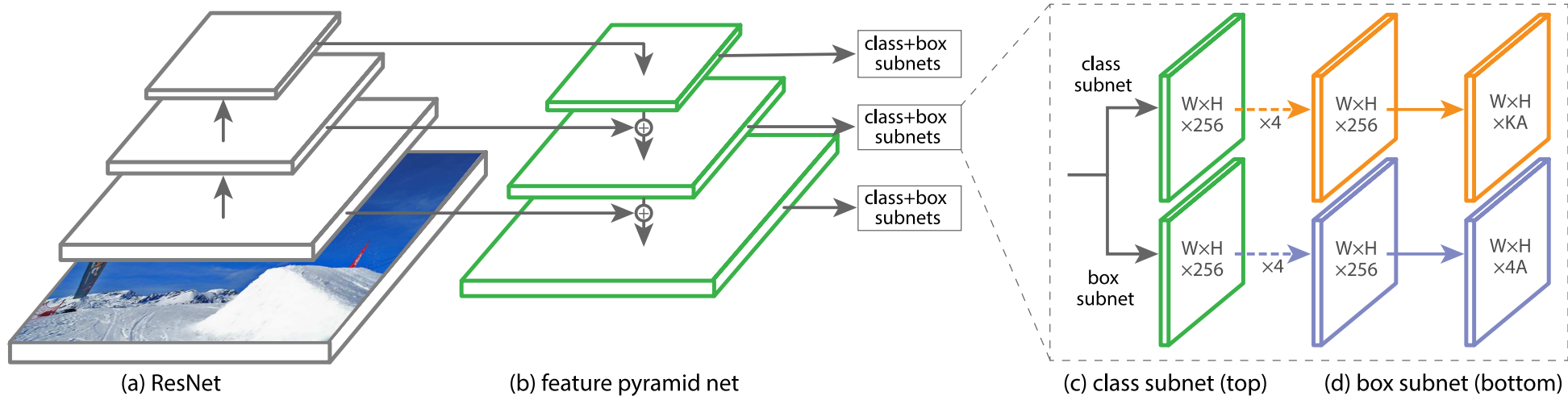


Figure 3 of "Focal Loss for Dense Object Detection", <https://arxiv.org/abs/1708.02002>

U.A.
fid · anchor

During training, anchors are assigned to ground-truth object boxes if IoU is at least 0.5; to background if IoU with any ground-truth region is at most 0.4 (the rest of anchors is ignored during training). The classification head is trained using focal loss with $\gamma = 2$ and $\alpha = 0.25$ (but according to the paper, all values of γ in $[0.5, 5]$ range work well); the boundary regression head is trained using smooth_{L_1} loss as in Fast(er) R-CNN.

During inference, at most 1000 objects with at least 5% probability from all pyramid levels are considered, and all of them are combined using non-maximum suppression with a threshold of 0.5. Fixed-size training and testing is used, with sizes 400, 500, ..., 800 pixels.

| | backbone | AP | AP ₅₀ | AP ₇₅ | AP _S | AP _M | AP _L |
|----------------------------|--------------------------|-------------|------------------|------------------|-----------------|-----------------|-----------------|
| <i>Two-stage methods</i> | | | | | | | |
| Faster R-CNN+++ [16] | ResNet-101-C4 | 34.9 | 55.7 | 37.4 | 15.6 | 38.7 | 50.9 |
| Faster R-CNN w FPN [20] | ResNet-101-FPN | 36.2 | 59.1 | 39.0 | 18.2 | 39.0 | 48.2 |
| Faster R-CNN by G-RMI [17] | Inception-ResNet-v2 [34] | 34.7 | 55.5 | 36.7 | 13.5 | 38.1 | 52.0 |
| Faster R-CNN w TDM [32] | Inception-ResNet-v2-TDM | 36.8 | 57.7 | 39.2 | 16.2 | 39.8 | 52.1 |
| <i>One-stage methods</i> | | | | | | | |
| YOLOv2 [27] | DarkNet-19 [27] | 21.6 | 44.0 | 19.2 | 5.0 | 22.4 | 35.5 |
| SSD513 [22, 9] | ResNet-101-SSD | 31.2 | 50.4 | 33.3 | 10.2 | 34.5 | 49.8 |
| DSSD513 [9] | ResNet-101-DSSD | 33.2 | 53.3 | 35.2 | 13.0 | 35.4 | 51.1 |
| RetinaNet (ours) | ResNet-101-FPN | 39.1 | 59.1 | 42.3 | 21.8 | 42.7 | 50.2 |
| RetinaNet (ours) | ResNeXt-101-FPN | 40.8 | 61.1 | 44.1 | 24.1 | 44.2 | 51.2 |

Table 2 of "Focal Loss for Dense Object Detection", <https://arxiv.org/abs/1708.02002>

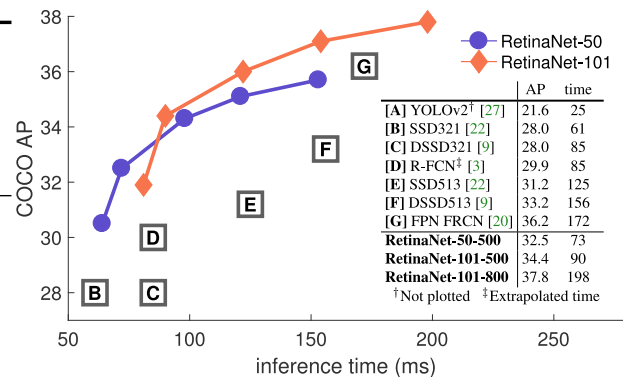


Figure 2 of "Focal Loss for Dense Object Detection", <https://arxiv.org/abs/1708.02002>

Ablations use ResNet-50-FPN backbone trained and tested with 600-pixel images.

| α | AP | AP ₅₀ | AP ₇₅ | γ | α | AP | AP ₅₀ | AP ₇₅ | #sc | #ar | AP | AP ₅₀ | AP ₇₅ |
|----------|------|------------------|------------------|----------|----------|-------------|------------------|------------------|-----|-----|-------------|------------------|------------------|
| .10 | 0.0 | 0.0 | 0.0 | 0 | .75 | 31.1 | 49.4 | 33.0 | 1 | 1 | 30.3 | 49.0 | 31.8 |
| .25 | 10.8 | 16.0 | 11.7 | 0.1 | .75 | 31.4 | 49.9 | 33.1 | 2 | 1 | 31.9 | 50.0 | 34.0 |
| .50 | 30.2 | 46.7 | 32.8 | 0.2 | .75 | 31.9 | 50.7 | 33.4 | 3 | 1 | 31.8 | 49.4 | 33.7 |
| .75 | 31.1 | 49.4 | 33.0 | 0.5 | .50 | 32.9 | 51.7 | 35.2 | 1 | 3 | 32.4 | 52.3 | 33.9 |
| .90 | 30.8 | 49.7 | 32.3 | 1.0 | .25 | 33.7 | 52.0 | 36.2 | 2 | 3 | 34.2 | 53.1 | 36.5 |
| .99 | 28.7 | 47.4 | 29.9 | 2.0 | .25 | 34.0 | 52.5 | 36.5 | 3 | 3 | 34.0 | 52.5 | 36.5 |
| .999 | 25.1 | 41.7 | 26.1 | 5.0 | .25 | 32.2 | 49.6 | 34.8 | 4 | 3 | 33.8 | 52.1 | 36.2 |

(a) Varying α for CE loss ($\gamma = 0$) (b) Varying γ for FL (w. optimal α) (c) Varying anchor scales and aspects

| method | batch size | nms thr | AP | AP ₅₀ | AP ₇₅ | depth | scale | AP | AP ₅₀ | AP ₇₅ | AP _S | AP _M | AP _L | time |
|-----------|------------|---------|-------------|------------------|------------------|-------|-------|------|------------------|------------------|-----------------|-----------------|-----------------|------|
| OHEM | 128 | .7 | 31.1 | 47.2 | 33.2 | 50 | 400 | 30.5 | 47.8 | 32.7 | 11.2 | 33.8 | 46.1 | 64 |
| OHEM | 256 | .7 | 31.8 | 48.8 | 33.9 | 50 | 500 | 32.5 | 50.9 | 34.8 | 13.9 | 35.8 | 46.7 | 72 |
| OHEM | 512 | .7 | 30.6 | 47.0 | 32.6 | 50 | 600 | 34.3 | 53.2 | 36.9 | 16.2 | 37.4 | 47.4 | 98 |
| OHEM | 128 | .5 | 32.8 | 50.3 | 35.1 | 50 | 700 | 35.1 | 54.2 | 37.7 | 18.0 | 39.3 | 46.4 | 121 |
| OHEM | 256 | .5 | 31.0 | 47.4 | 33.0 | 50 | 800 | 35.7 | 55.0 | 38.5 | 18.9 | 38.9 | 46.3 | 153 |
| OHEM | 512 | .5 | 27.6 | 42.0 | 29.2 | 101 | 400 | 31.9 | 49.5 | 34.1 | 11.6 | 35.8 | 48.5 | 81 |
| OHEM 1:3 | 128 | .5 | 31.1 | 47.2 | 33.2 | 101 | 500 | 34.4 | 53.1 | 36.8 | 14.7 | 38.5 | 49.1 | 90 |
| OHEM 1:3 | 256 | .5 | 28.3 | 42.4 | 30.3 | 101 | 600 | 36.0 | 55.2 | 38.7 | 17.4 | 39.6 | 49.7 | 122 |
| OHEM 1:3 | 512 | .5 | 24.0 | 35.5 | 25.8 | 101 | 700 | 37.1 | 56.6 | 39.8 | 19.1 | 40.6 | 49.4 | 154 |
| FL | n/a | n/a | 36.0 | 54.9 | 38.7 | 101 | 800 | 37.8 | 57.5 | 40.8 | 20.2 | 41.1 | 49.2 | 198 |

(d) FL vs. OHEM baselines (with ResNet-101-FPN) (e) Accuracy/speed trade-off RetinaNet (on test-dev)

Table 1 of "Focal Loss for Dense Object Detection", <https://arxiv.org/abs/1708.02002>

EfficientDet – Architecture

EfficientDet builds up on EfficientNet and delivered state-of-the-art performance in Nov 2019 with minimum time and space requirements (however, its performance has already been surpassed significantly). It is a single-scale detector similar to RetinaNet, which:

- uses EfficientNet as a backbone;
- employs compound scaling;
- uses a newly proposed BiFPN, “efficient bidirectional cross-scale connections and weighted feature fusion”.

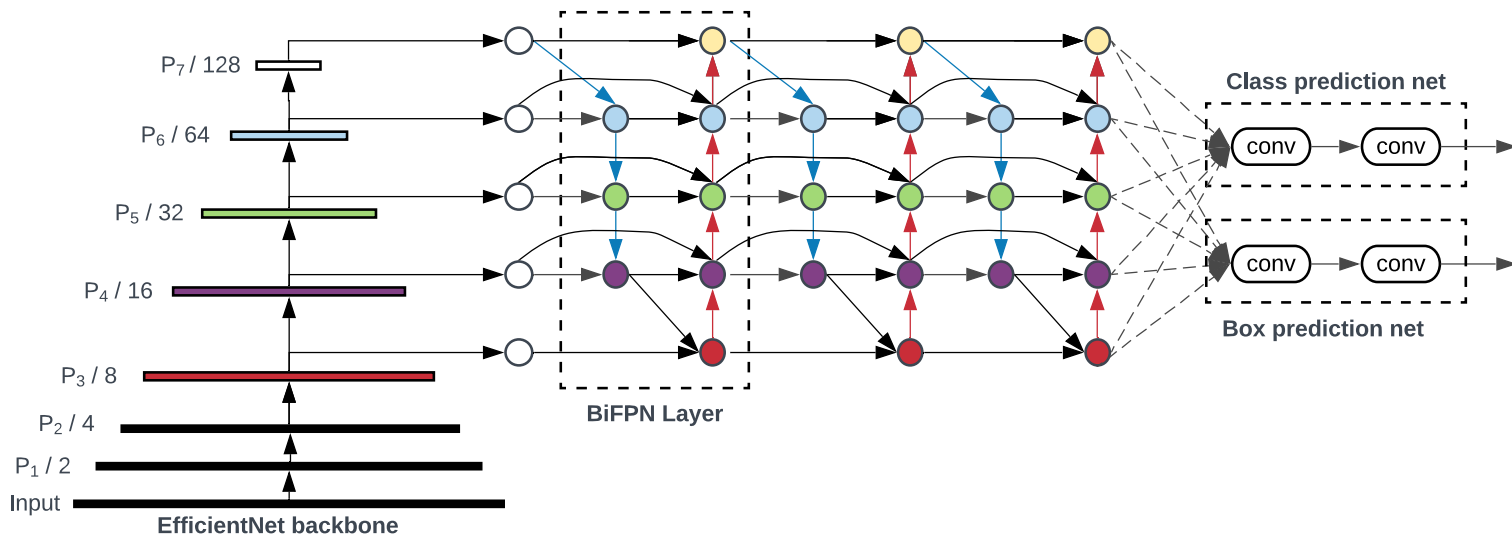


Figure 3 of "EfficientDet: Scalable and Efficient Object Detection", <https://arxiv.org/abs/1911.09070>

In multi-scale fusion in FPN, information flows only from the pyramid levels with smaller resolution to the levels with higher resolution.

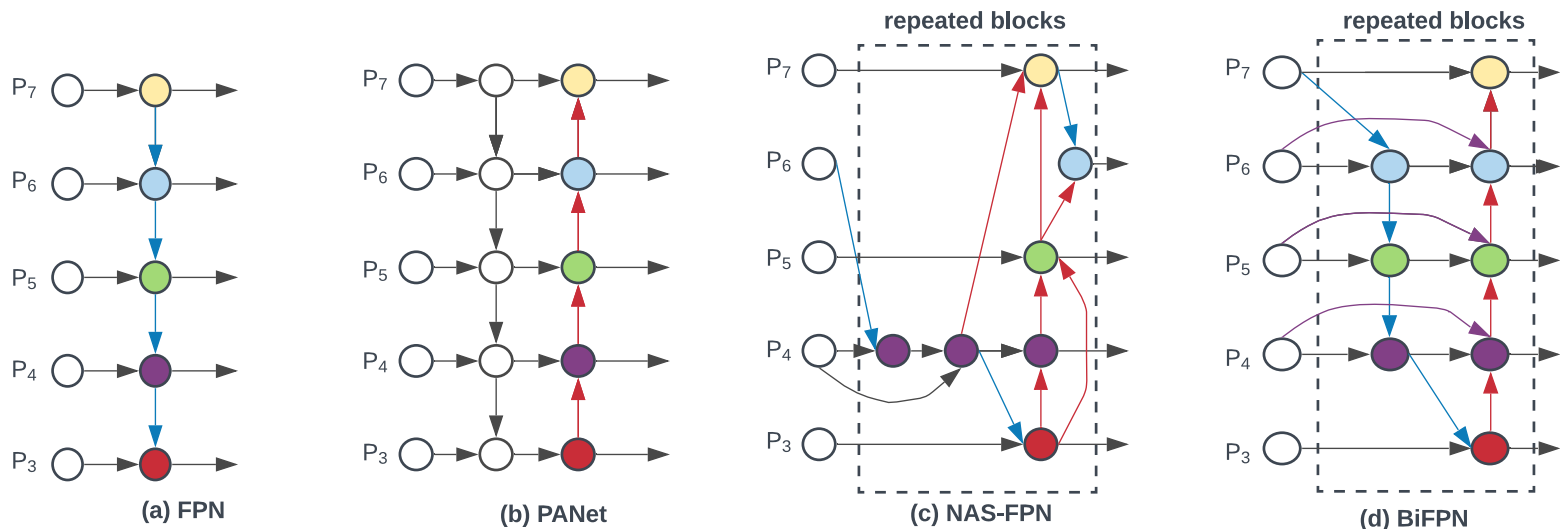


Figure 2 of "EfficientDet: Scalable and Efficient Object Detection", <https://arxiv.org/abs/1911.09070>

BiFPN consists of several rounds of bidirectional flows. Each bidirectional flow employs residual connections and does not include nodes that have only one input edge with no feature fusion. All operations are 3×3 separable convolutions with batch normalization and ReLU, upsampling is done by repeating rows and columns and downsampling by max-pooling.

When combining features with different resolutions, it is common to resize them to the same resolution and sum them – therefore, all set of features are considered to be of the same importance. The authors however argue that features from different resolution contribute to the final result *unequally* and propose to combine them with trainable weights.

- **Softmax-based fusion:** In each BiFPN node, we create a trainable weight w_i for every input \mathbf{l}_i and the final combination (after resize, before a convolution) is

$$\sum_i \frac{e^{w_i}}{\sum_j e^{w_j}} \mathbf{l}_i.$$

- **Fast normalized fusion:** Authors propose a simpler alternative of weighting:

$$\sum_i \frac{\text{ReLU}(w_i)}{\varepsilon + \sum_j \text{ReLU}(w_j)} \mathbf{l}_i.$$

It uses $\varepsilon = 0.0001$ for stability and is up to 30% faster on a GPU.

EfficientDet – Compound Scaling

Similar to EfficientNet, authors propose to scale various dimensions of the network, using a single compound coefficient ϕ .

After performing a grid search:

- the width of BiFPN is scaled as $W_{BiFPN} = 64 \cdot 1.35^\phi$,
- the depth of BiFPN is scaled as $D_{BiFPN} = 3 + \phi$,
- the box/class predictor has the same width as BiFPN and depth $D_{class} = 3 + \lfloor \phi/3 \rfloor$,
- input image resolution increases according to $R_{image} = 512 + 128 \cdot \phi$.

| | Input size R_{input} | Backbone Network | BiFPN | | Box/class |
|-------------------|------------------------------|---------------------|--------------------------|------------------------|------------------------|
| | | | #channels W_{bifpn} | #layers D_{bifpn} | #layers D_{class} |
| D0 ($\phi = 0$) | 512 | B0 | 64 | 3 | 3 |
| D1 ($\phi = 1$) | 640 | B1 | 88 | 4 | 3 |
| D2 ($\phi = 2$) | 768 | B2 | 112 | 5 | 3 |
| D3 ($\phi = 3$) | 896 | B3 | 160 | 6 | 4 |
| D4 ($\phi = 4$) | 1024 | B4 | 224 | 7 | 4 |
| D5 ($\phi = 5$) | 1280 | B5 | 288 | 7 | 4 |
| D6 ($\phi = 6$) | 1280 | B6 | 384 | 8 | 5 |
| D6 ($\phi = 7$) | 1536 | B6 | 384 | 8 | 5 |

Table 1 of "EfficientDet: Scalable and Efficient Object Detection", <https://arxiv.org/abs/1911.09070>

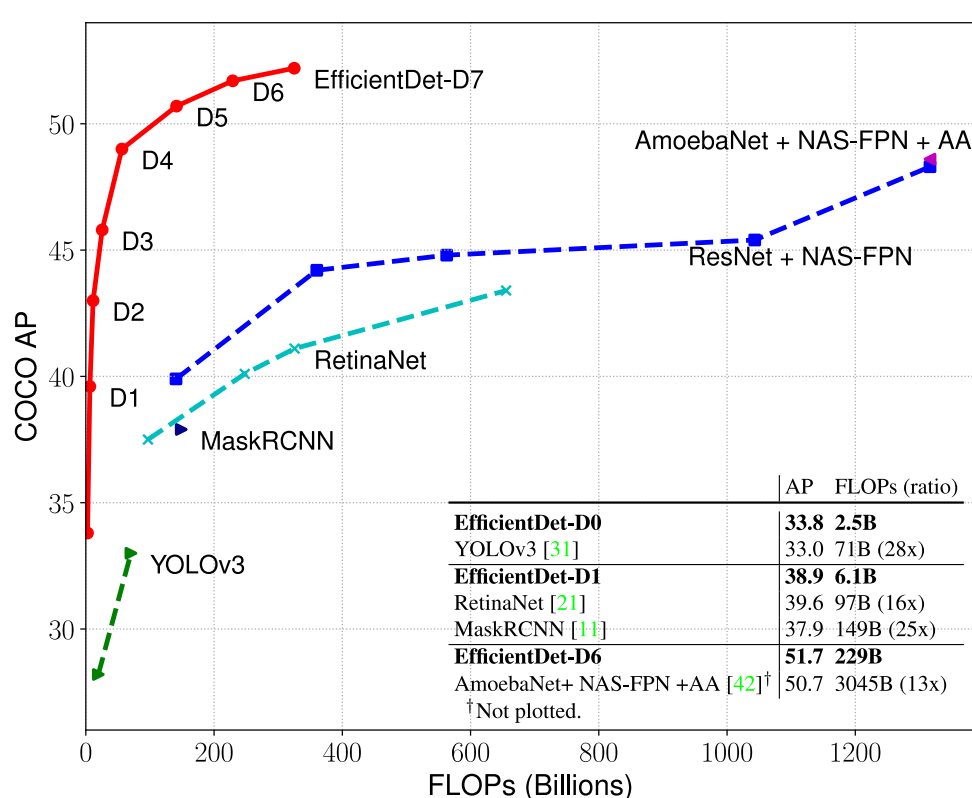


Figure 1 of "EfficientDet: Scalable and Efficient Object Detection", <https://arxiv.org/abs/1911.09070>

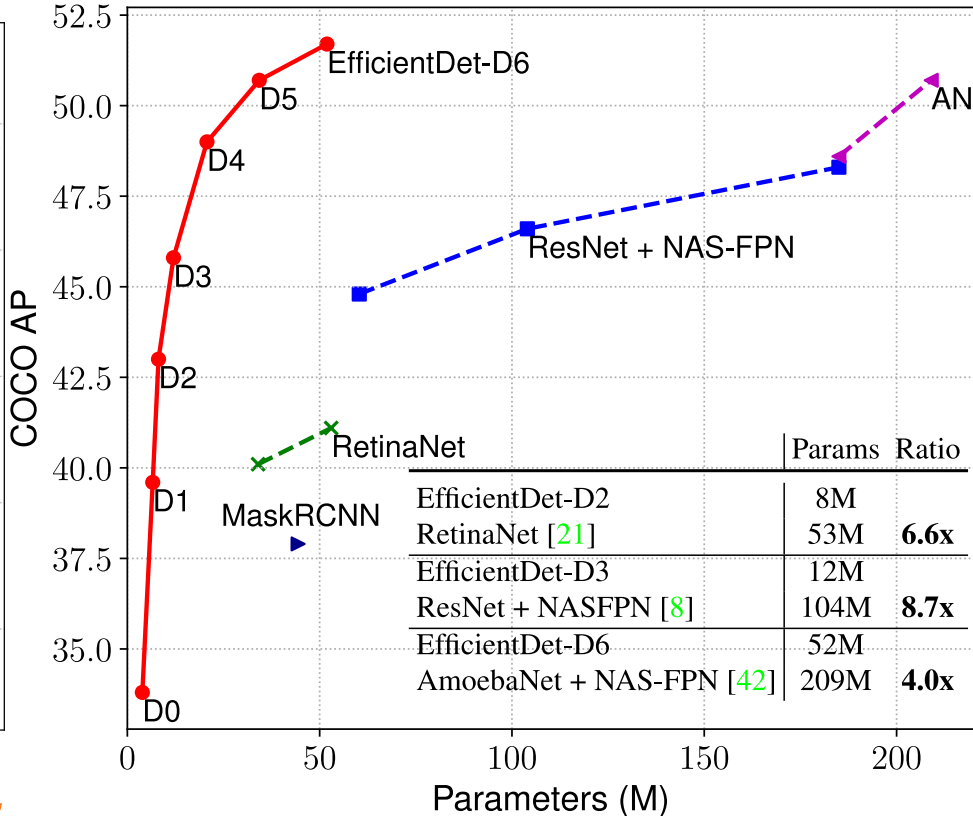


Figure 4 of "EfficientDet: Scalable and Efficient Object Detection", <https://arxiv.org/abs/1911.09070>

| Model | tet-dev | | | val | Params | Ratio | FLOPs | Ratio | Latency | |
|-----------------------------------|-------------|-------------|-------------|-------------|-------------|-----------|-------------|-----------|-------------------|------------------|
| | AP | AP_{50} | AP_{75} | AP | | | | | GPU _{ms} | CPU _s |
| EfficientDet-D0 (512) | 33.8 | 52.2 | 35.8 | 33.5 | 3.9M | 1x | 2.5B | 1x | 16 | 0.32 |
| YOLOv3 [31] | 33.0 | 57.9 | 34.4 | - | - | - | 71B | 28x | 51 [†] | - |
| EfficientDet-D1 (640) | 39.6 | 58.6 | 42.3 | 39.1 | 6.6M | 1x | 6.1B | 1x | 20 | 0.74 |
| RetinaNet-R50 (640) [21] | 37.0 | - | - | - | 34M | 6.7x | 97B | 16x | 27 | 2.8 |
| RetinaNet-R101 (640)[21] | 37.9 | - | - | - | 53M | 8.0x | 127B | 21x | 34 | 3.6 |
| EfficientDet-D2 (768) | 43.0 | 62.3 | 46.2 | 42.5 | 8.1M | 1x | 11B | 1x | 24 | 1.2 |
| RetinaNet-R50 (1024) [21] | 40.1 | - | - | - | 34M | 4.3x | 248B | 23x | 51 | 7.5 |
| RetinaNet-R101 (1024) [21] | 41.1 | - | - | - | 53M | 6.6x | 326B | 30x | 65 | 9.7 |
| ResNet-50 + NAS-FPN (640) [8] | 39.9 | - | - | - | 60M | 7.5x | 141B | 13x | 41 | 4.1 |
| EfficientDet-D3 (896) | 45.8 | 65.0 | 49.3 | 45.9 | 12M | 1x | 25B | 1x | 42 | 2.5 |
| ResNet-50 + NAS-FPN (1024) [8] | 44.2 | - | - | - | 60M | 5.1x | 360B | 15x | 79 | 11 |
| ResNet-50 + NAS-FPN (1280) [8] | 44.8 | - | - | - | 60M | 5.1x | 563B | 23x | 119 | 17 |
| ResNet-50 + NAS-FPN (1280@384)[8] | 45.4 | - | - | - | 104M | 8.7x | 1043B | 42x | 173 | 27 |
| EfficientDet-D4 (1024) | 49.4 | 69.0 | 53.4 | 49.0 | 21M | 1x | 55B | 1x | 74 | 4.8 |
| AmoebaNet+ NAS-FPN +AA(1280)[42] | - | - | - | 48.6 | 185M | 8.8x | 1317B | 24x | 259 | 38 |
| EfficientDet-D5 (1280) | 50.7 | 70.2 | 54.7 | 50.5 | 34M | 1x | 135B | 1x | 141 | 11 |
| EfficientDet-D6 (1280) | 51.7 | 71.2 | 56.0 | 51.3 | 52M | 1x | 226B | 1x | 190 | 16 |
| AmoebaNet+ NAS-FPN +AA(1536)[42] | - | - | - | 50.7 | 209M | 4.0x | 3045B | 13x | 608 | 83 |
| EfficientDet-D7 (1536) | 52.2 | 71.4 | 56.3 | 51.8 | 52M | 1x | 325B | 1x | 262 | 24 |

We omit ensemble and test-time multi-scale results [27, 10].

[†]Latency marked with [†] are from papers, and others are measured on the same machine with Titan V GPU.

Table 2 of "EfficientDet: Scalable and Efficient Object Detection", <https://arxiv.org/abs/1911.09070>

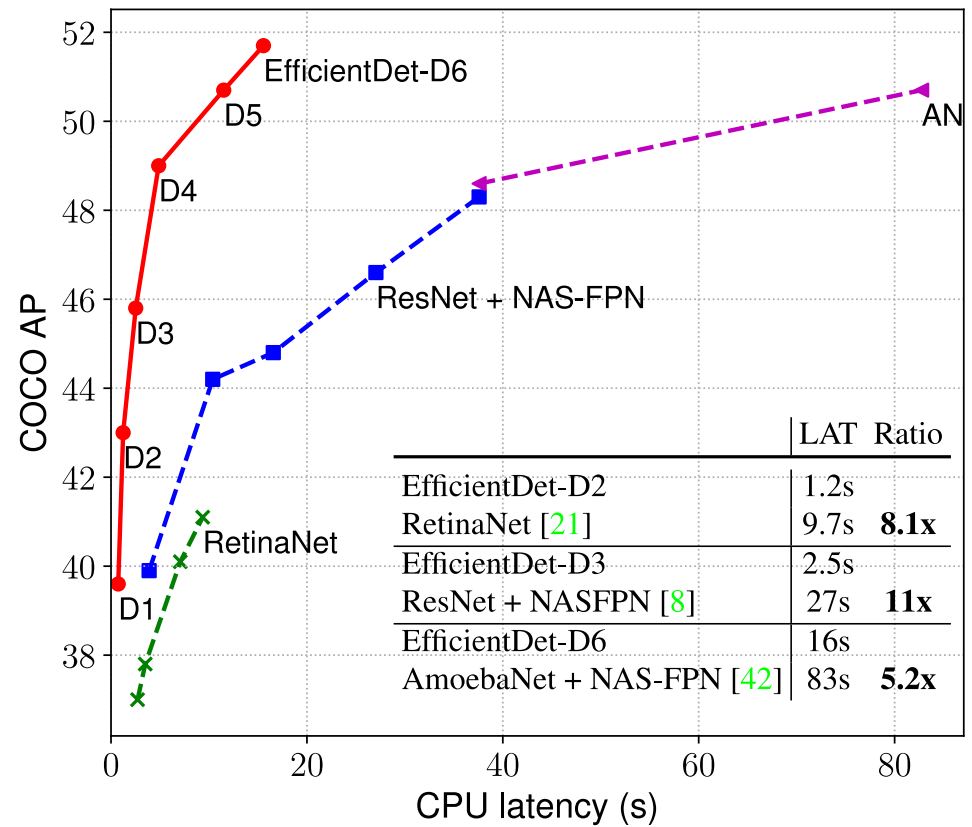
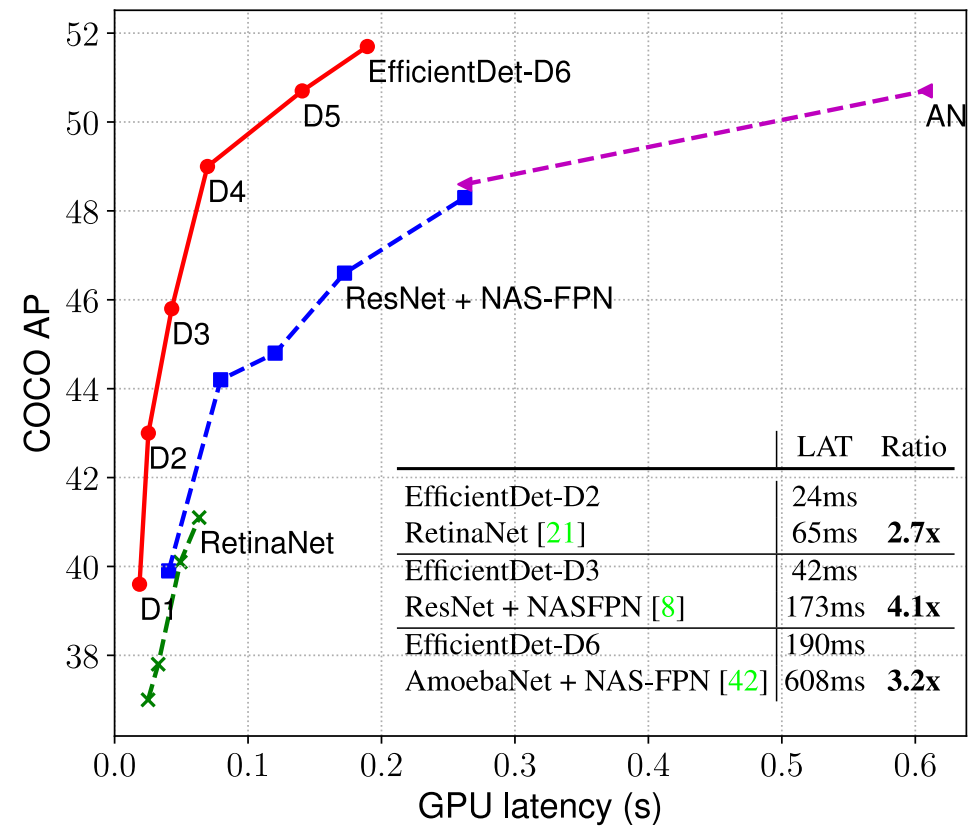


Figure 4 of "EfficientDet: Scalable and Efficient Object Detection", <https://arxiv.org/abs/1911.09070>

Given that EfficientDet employs both a powerful backbone and new BiFPN, authors quantify the improvement of the individual components.

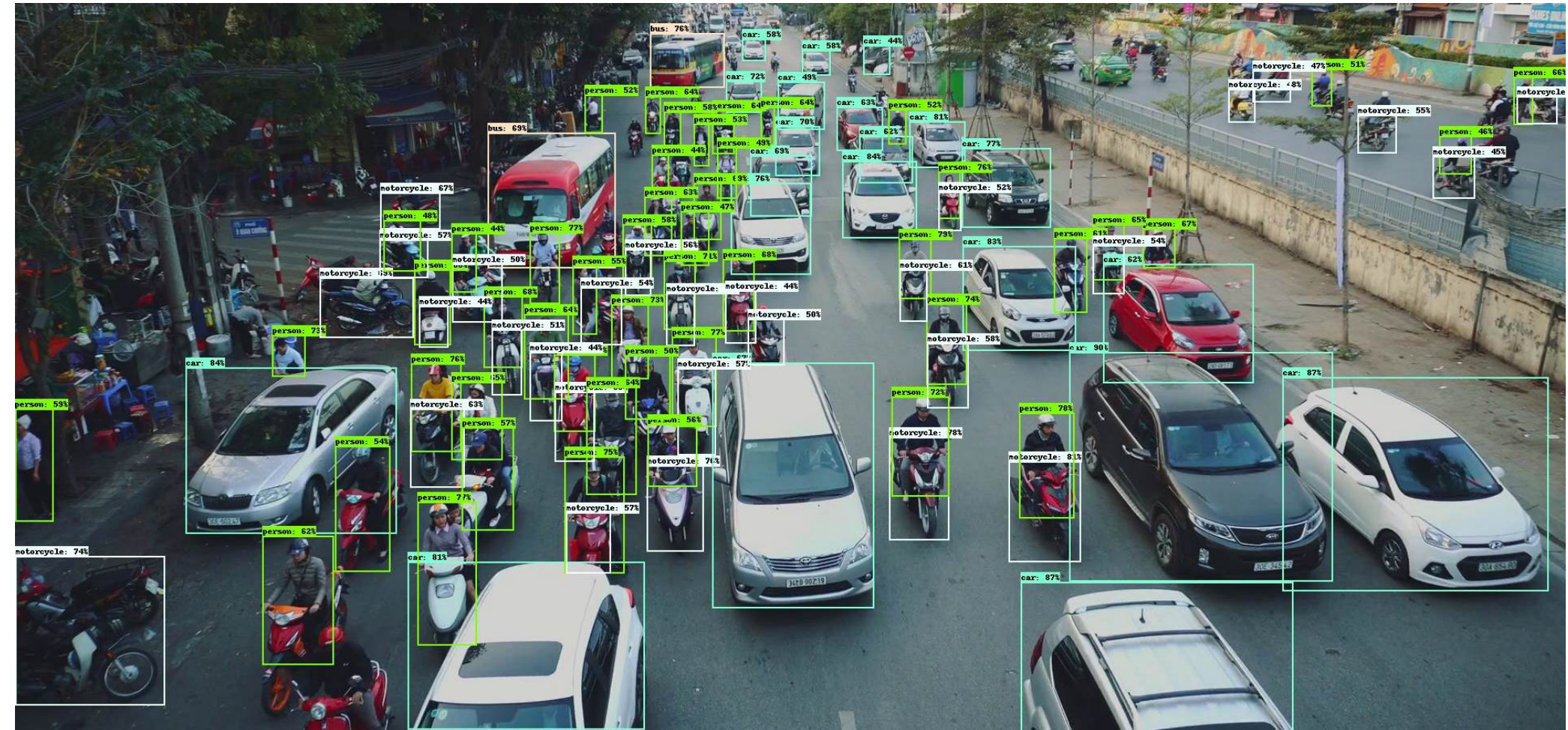
| | AP | Parameters | FLOPs |
|---------------------------------------|------|------------|-------|
| ResNet50 + FPN | 37.0 | 34M | 97B |
| EfficientNet-B3 + FPN | 40.3 | 21M | 75B |
| EfficientNet-B3 + BiFPN | 44.4 | 12M | 24B |

Table 4 of "EfficientDet: Scalable and Efficient Object Detection", <https://arxiv.org/abs/1911.09070>

The comparison with previously used cross-scale fusion architectures is also provided:

| | AP | #Params ratio | #FLOPs ratio |
|-----------------------------|--------------|------------------|-----------------|
| Repeated top-down FPN | 42.29 | 1.0x | 1.0x |
| Repeated FPN+PANet | 44.08 | 1.0x | 1.0x |
| NAS-FPN | 43.16 | 0.71x | 0.72x |
| Fully-Connected FPN | 43.06 | 1.24x | 1.21x |
| BiFPN (w/o weighted) | 43.94 | 0.88x | 0.67x |
| BiFPN (w/ weighted) | 44.39 | 0.88x | 0.68x |

Table 5 of "EfficientDet: Scalable and Efficient Object Detection", <https://arxiv.org/abs/1911.09070>



<https://github.com/google/automl/blob/master/efficientdet/g3doc/street.jpg>

Batch Normalization *→ je na nie, pretože je to moc malý (obrázok je to ešte len jednotky)*

Neuron value is normalized across the minibatch, and in case of CNN also across all positions.

Layer Normalization

Neuron value is normalized across the layer.

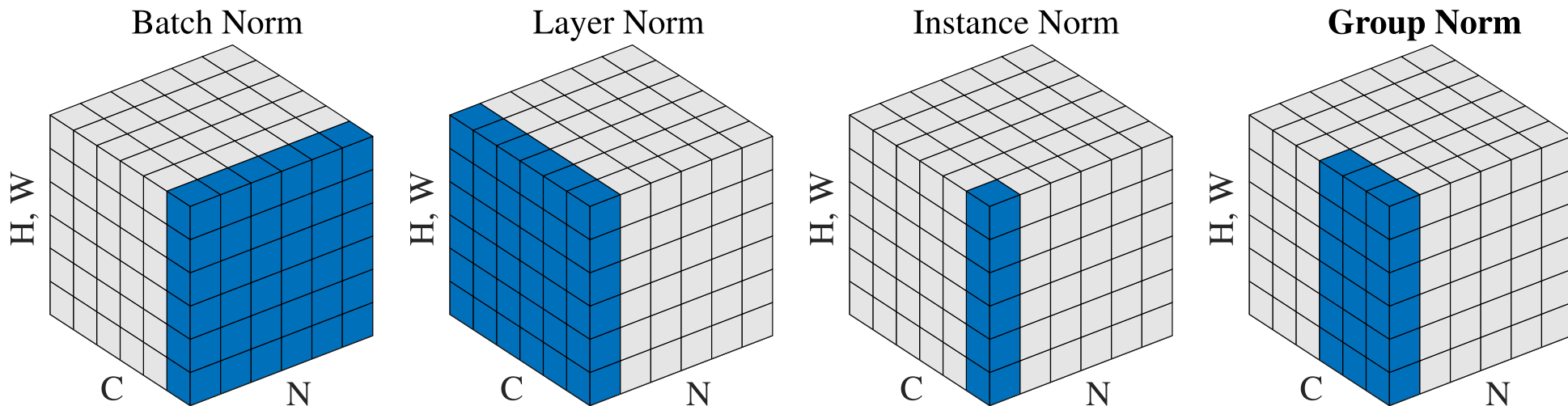
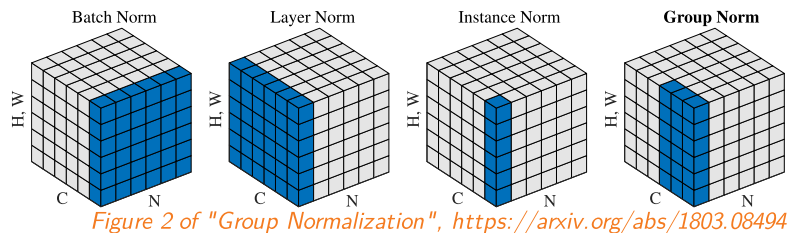


Figure 2 of "Group Normalization", <https://arxiv.org/abs/1803.08494>

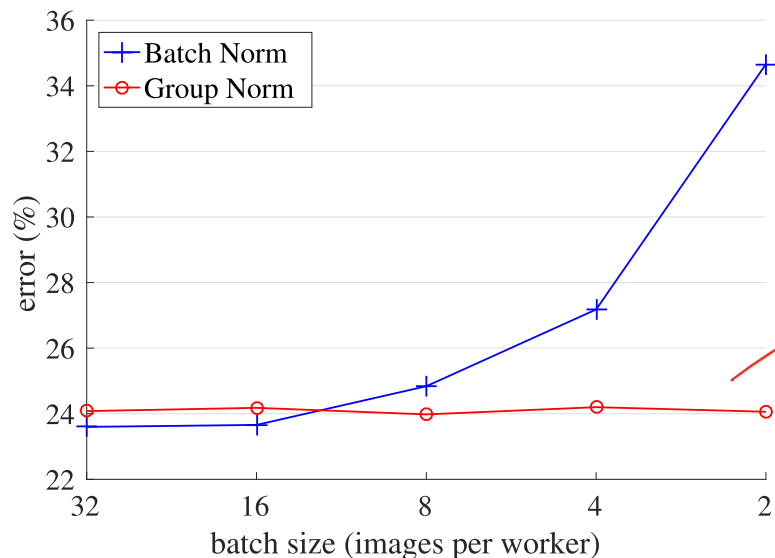
Group Normalization

Group Normalization is analogous to Layer normalization, but the channels are normalized in groups (by default, $G = 32$).

Osoboďm se o veľkosti
batchu a veľkosti batchu
presnosť



to je dôležité u fine
tuningu veľkého modelu.



sie tréba hoxť na
veľkom batchu, ale dôležité
byť na malých batchoch

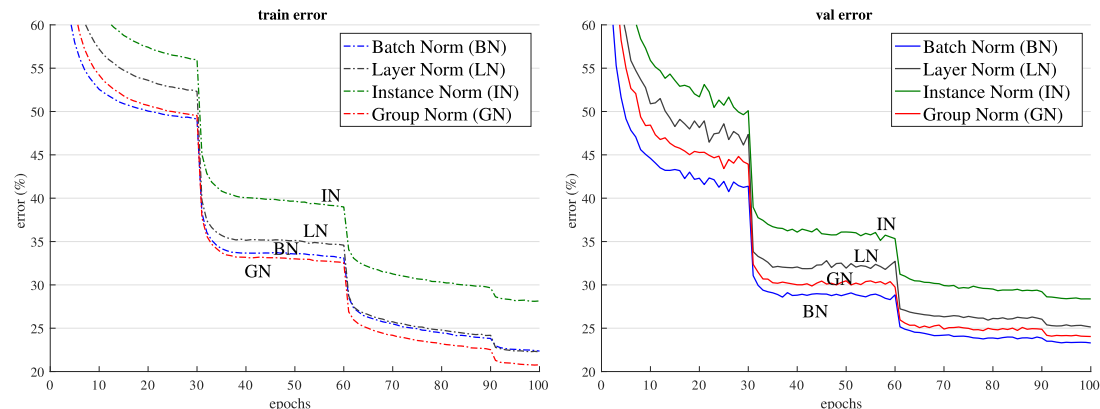


Figure 4. Comparison of error curves with a batch size of 32 images/GPU. We show the ImageNet training error (left) and validation error (right) vs. numbers of training epochs. The model is ResNet-50.

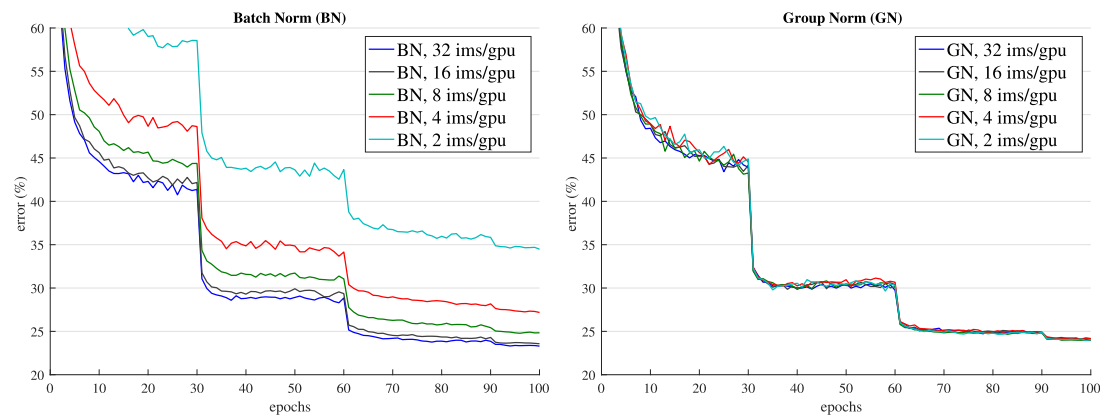


Figure 5. Sensitivity to batch sizes: ResNet-50's validation error of BN (left) and GN (right) trained with 32, 16, 8, 4, and 2 images/GPU.

Figures 4 and 5 of "Group Normalization", <https://arxiv.org/abs/1803.08494>

| backbone | AP^{bbox} | AP_{50}^{bbox} | AP_{75}^{bbox} | AP^{mask} | AP_{50}^{mask} | AP_{75}^{mask} |
|----------|-------------|------------------|------------------|-------------|------------------|------------------|
| BN* | 37.7 | 57.9 | 40.9 | 32.8 | 54.3 | 34.7 |
| GN | 38.8 | 59.2 | 42.2 | 33.6 | 55.9 | 35.4 |

Table 4. **Detection and segmentation results in COCO**, using Mask R-CNN with **ResNet-50 C4**. BN* means BN is frozen.

| backbone | box head | AP^{bbox} | AP_{50}^{bbox} | AP_{75}^{bbox} | AP^{mask} | AP_{50}^{mask} | AP_{75}^{mask} |
|----------|----------|-------------|------------------|------------------|-------------|------------------|------------------|
| BN* | - | 38.6 | 59.5 | 41.9 | 34.2 | 56.2 | 36.1 |
| BN* | GN | 39.5 | 60.0 | 43.2 | 34.4 | 56.4 | 36.3 |
| GN | GN | 40.0 | 61.0 | 43.3 | 34.8 | 57.3 | 36.3 |

Table 5. **Detection and segmentation results in COCO**, using Mask R-CNN with **ResNet-50 FPN** and a 4conv1fc bounding box head. BN* means BN is frozen.

Tables 4 and 5 of "Group Normalization", <https://arxiv.org/abs/1803.08494>